

Diagnosis of ENSO Related Air-Sea Feedbacks in Observations and Coupled GCMs

Tim Li

**Department of Atmospheric Sciences and IPRC
University of Hawaii**

What causes the growth of El Nino?

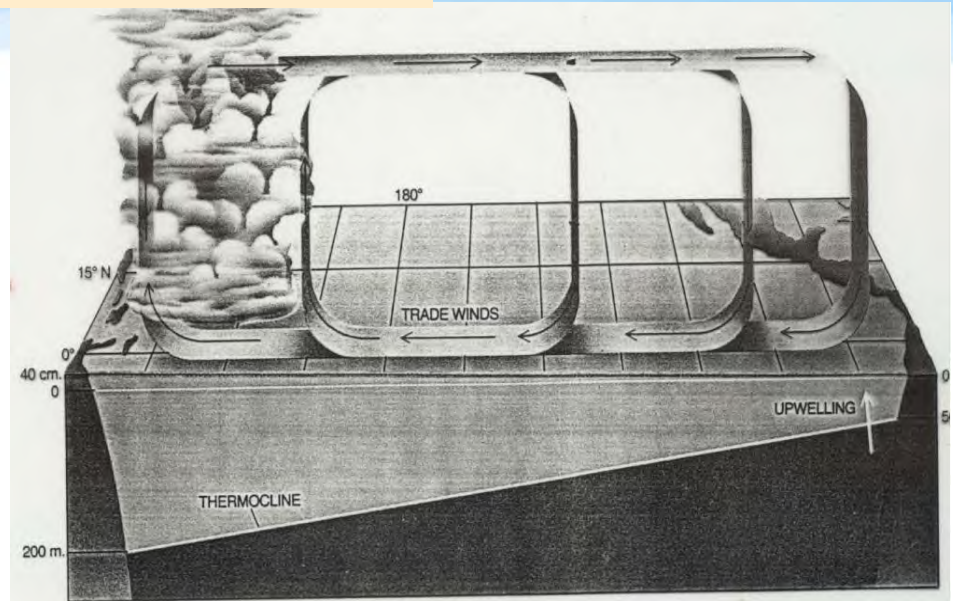
J. Bjerknes (1969) first termed the equatorial atmospheric zonal overturning circulation as “**Walker circulation**”.

Positive air-sea feedbacks:

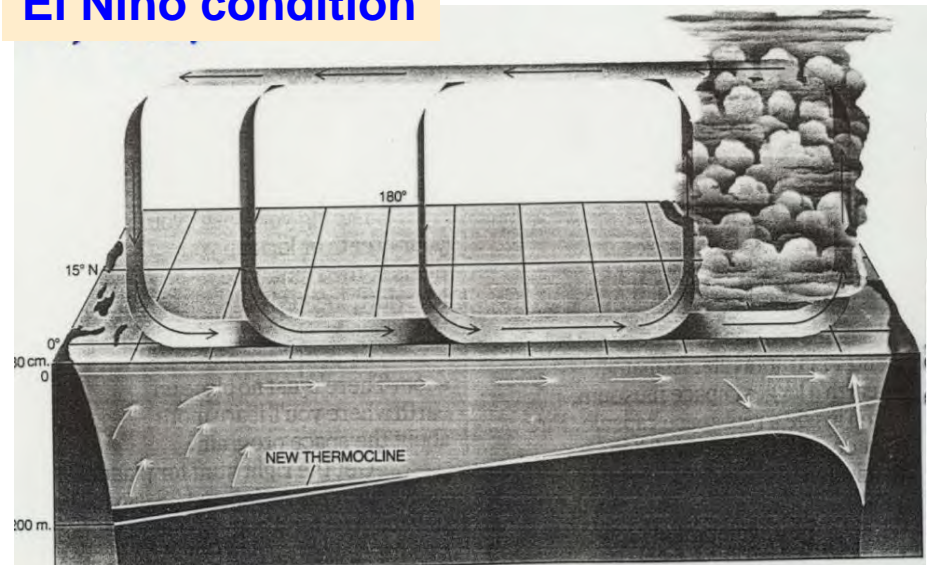
- Zonal advective feedback
- Ekman feedback
- Thermocline feedback

$$\frac{\partial T'}{\partial t} \approx -u'\bar{T}_x - w'\bar{T}_z - \bar{w}T'_z$$

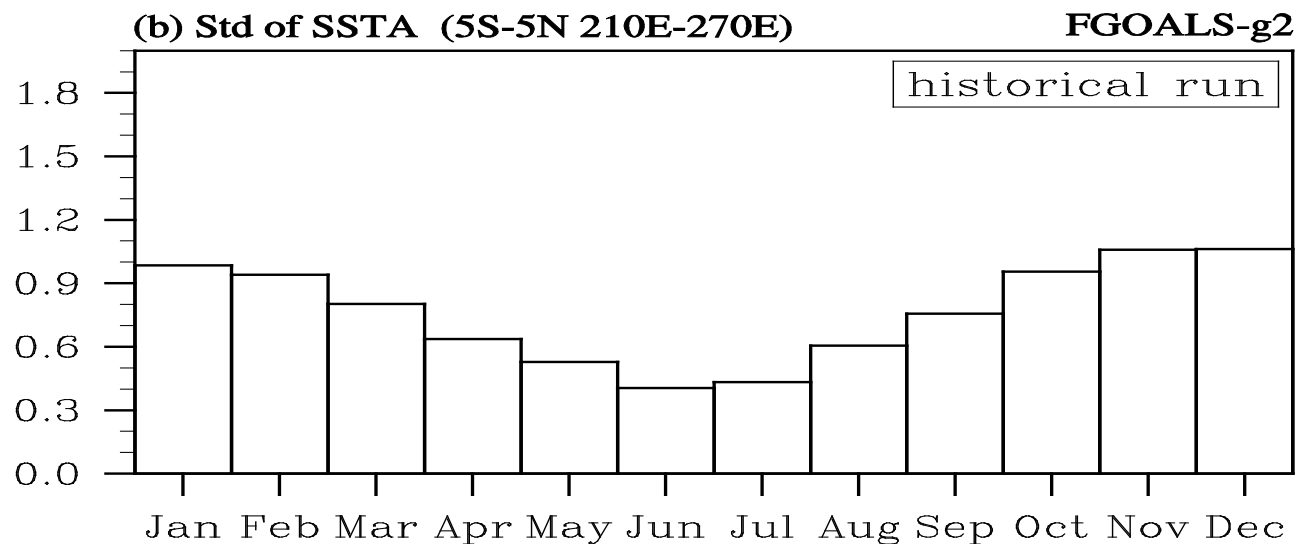
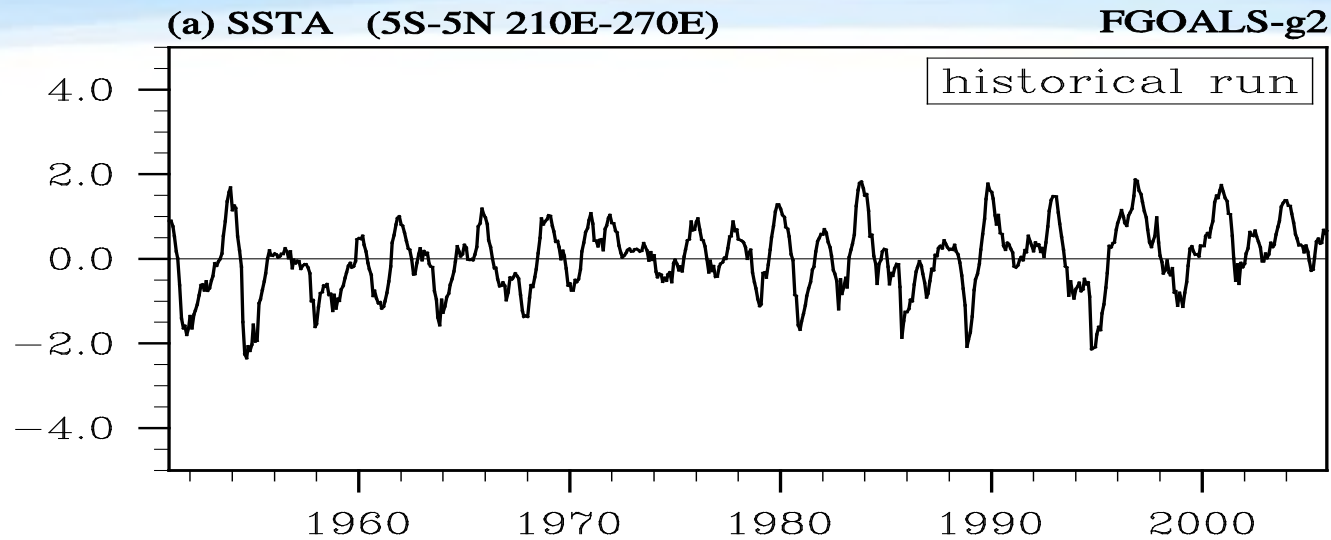
Normal condition



El Nino condition

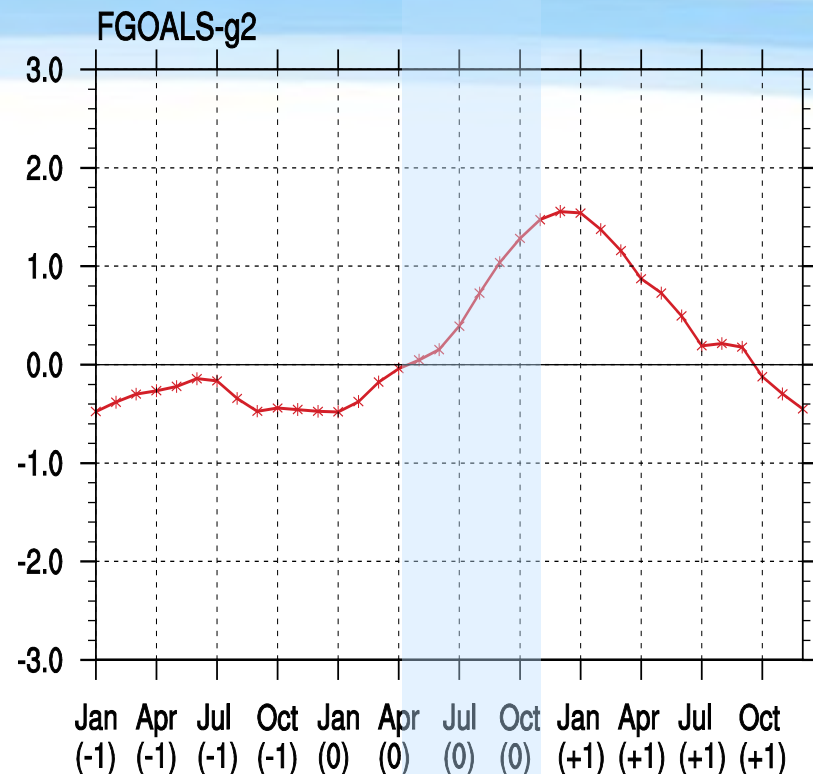
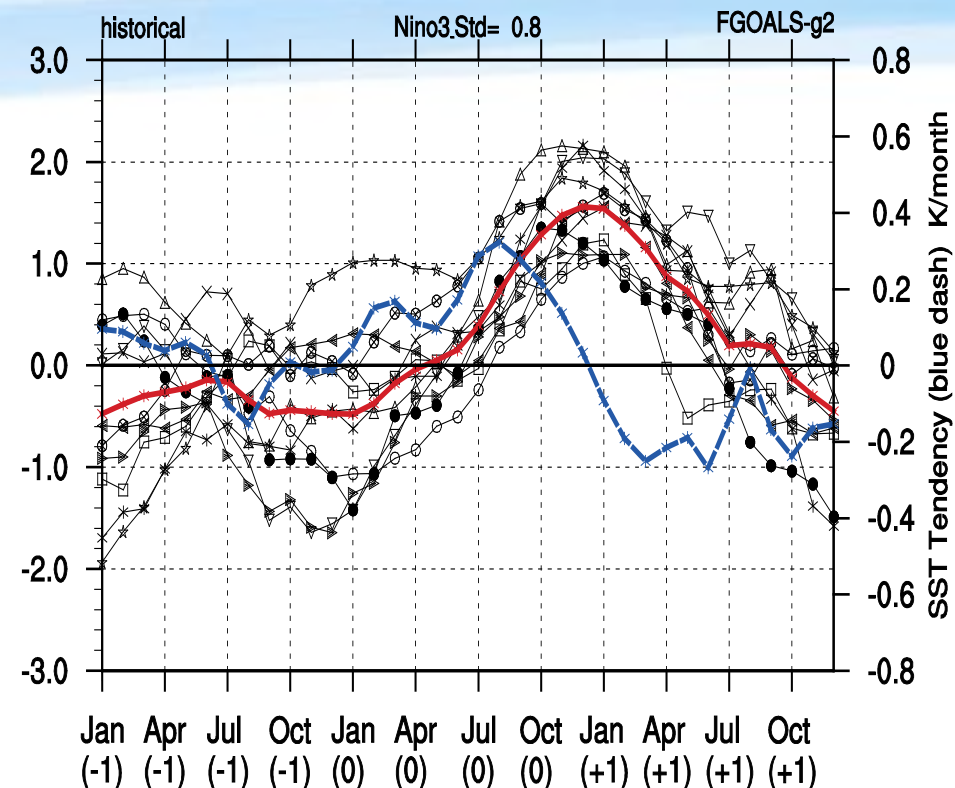


Example 1: Time series of Niño3 SSTA in FGOALS-G2



For given a coupled model, the ENSO strength might be weaker (or stronger) than the observed. How do you know which part of model air-sea feedback processes (atmospheric response to SST, ocean response to the wind, cloud radiative forcing, and/or surface latent heat flux) are incorrect?

Composite Time Series of SSTA in Nino3



- El Nino cases
- Composite El Nino case
- SSTA-tendency of the composite El Nino case

— Composite El Nino case

Diagnose the SSTA-tendency during **developing phase (Apr-Nov[0])** for composite El Nino

Mixed-layer temperature tendency equation

ML temperature tendency equation:

$$\begin{aligned}
 \frac{\partial T'}{\partial t} = & \underbrace{-u' \frac{\partial \bar{T}}{\partial x}}_{\text{term 1}} \underbrace{-\bar{u} \frac{\partial T'}{\partial x}}_{\text{term 2}} \underbrace{-u' \frac{\partial T'}{\partial x}}_{\text{term 3}} \underbrace{-w' \frac{\partial \bar{T}}{\partial z}}_{\text{term 4}} \underbrace{-\bar{w} \frac{\partial T'}{\partial z}}_{\text{term 5}} \underbrace{-w' \frac{\partial T'}{\partial z}}_{\text{term 6}} \\
 & \underbrace{-v' \frac{\partial \bar{T}}{\partial y}}_{\text{term 7}} \underbrace{-\bar{v} \frac{\partial T'}{\partial y}}_{\text{term 8}} \underbrace{-v' \frac{\partial T'}{\partial y}}_{\text{term 9}} + \underbrace{\frac{Q'_{net}}{\rho C_p H}}_{\text{term 10}} + R
 \end{aligned}$$

term 1 – term 10 are shown in the above equation

term 11: the sum of term1 to term 10;

term 12: the actual mixed layer temperature tendency

Bar: climatological seasonal cycle;

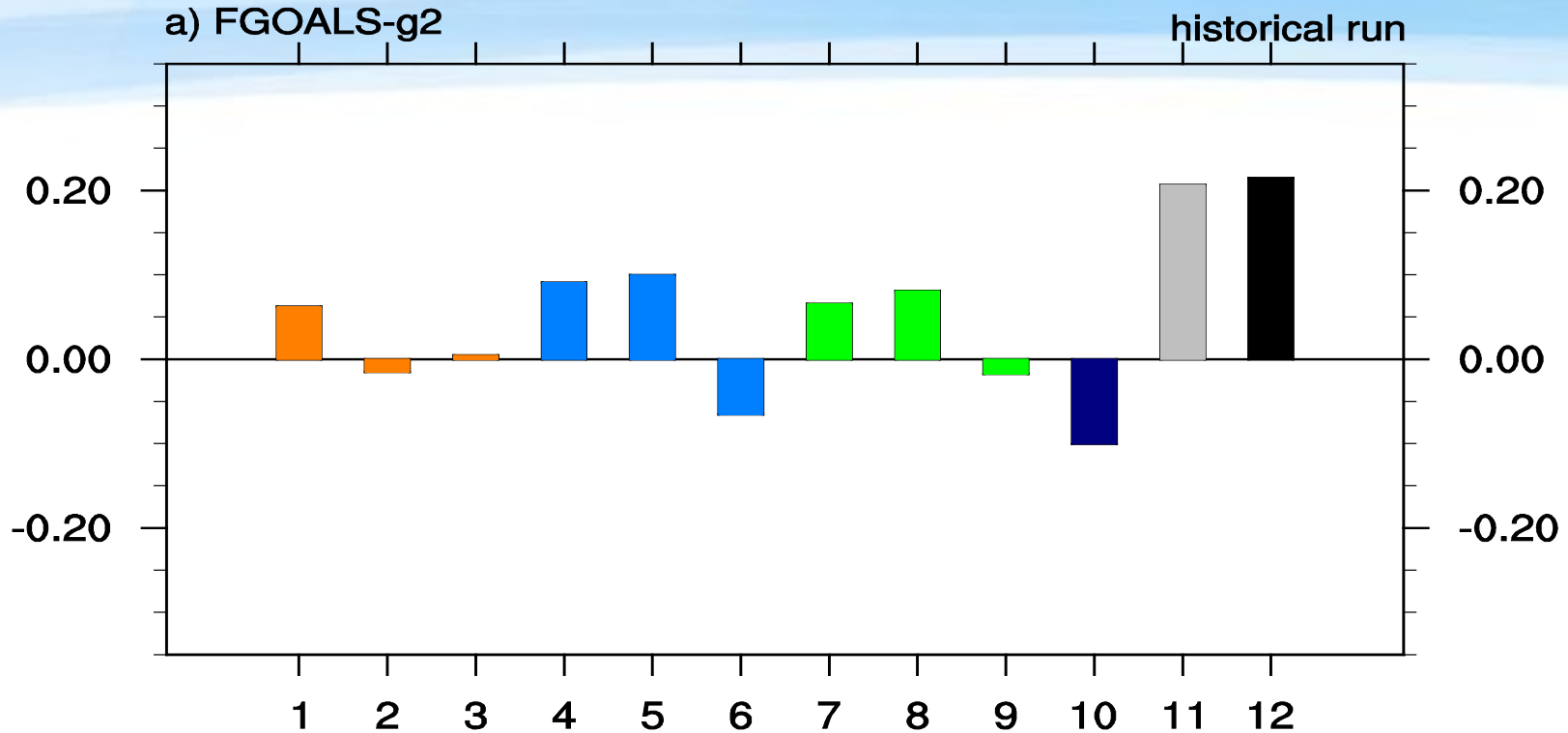
Prime: anomaly field with respect to the climatological seasonal cycle;

H: spatially and temporally varying mixed layer depth

R: residual term

$$Q_{net} = Q_{sw} - Q_{LW} - Q_{LH} - Q_{SH}$$

Mixed-Layer Heat Budget Diagnosis



The major contributing terms are **zonal advective feedback** (term 1), **Ekman feedback** (term 4), **thermocline feedback** (term 5) and **meridional advective feedback** (term 8)

$$\frac{\partial T'}{\partial t} = -\bar{w} \frac{T_e'}{h} - \frac{Q'}{\rho C_w h}$$

$$T' = \delta T e^{\sigma t}$$

$$\rho C_w h \sigma = -\rho C_w \bar{w} \frac{T_e'}{T'} - \frac{Q'}{T'}$$

$$BFI = \rho C_w \bar{w} R(u, T) R(D, u) R(T_e, D)$$

$$TFI = R(LHF, T) + R(SWR, T)$$

Combined dynamic and thermodynamic feedback index (CFI) may be written as:

$$**CFI = BFI + TFI**$$

Bjerkners Thermocline feedback

Following previous studies (Liu, Li, et al. 2012; Chen, Li, et al. 2015), the growth rate associated with thermocline feedback can be written as:

$$\sigma = \frac{\bar{w}}{H} R(\tau'_x, T') R(D', \tau'_x) R(T'_e, D')$$

\bar{w} : mean vertical velocity; H : mixed layer depth

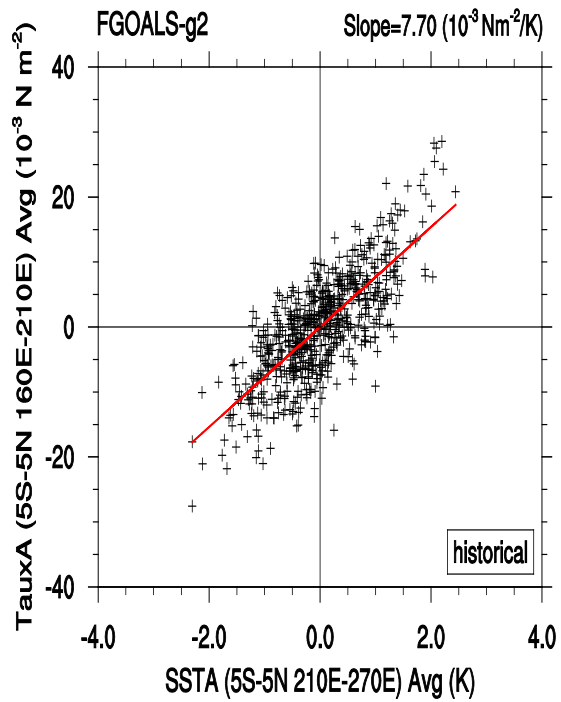
D' : thermocline depth anomaly; T'_e : subsurface ocean temperature anomaly

$R(\tau'_x, T')$: the atmospheric response of zonal wind stress anomaly (τ'_x) in the central equatorial Pacific (CEP) to a unit SSTA forcing in the eastern equatorial Pacific (EEP);

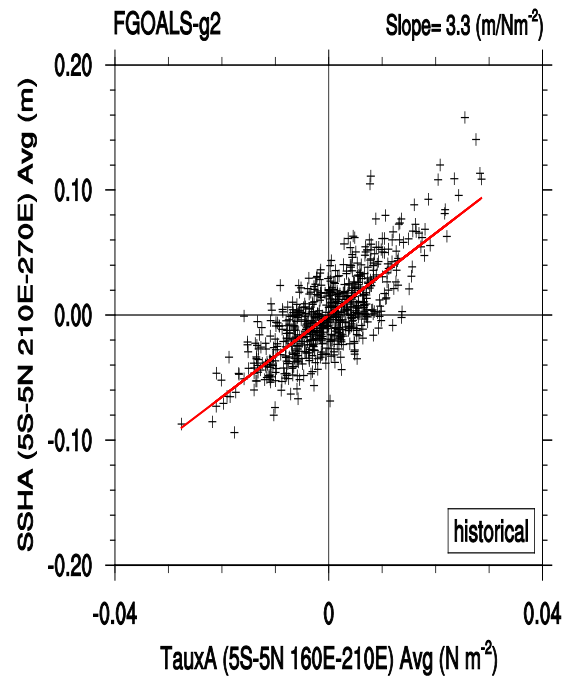
$R(D', \tau'_x)$: the response of ocean thermocline in EEP to a unit zonal wind stress (τ'_x) forcing in CEP;

$R(T'_e, D')$: the response of the ocean subsurface temperature to a unit thermocline depth change in EEP.

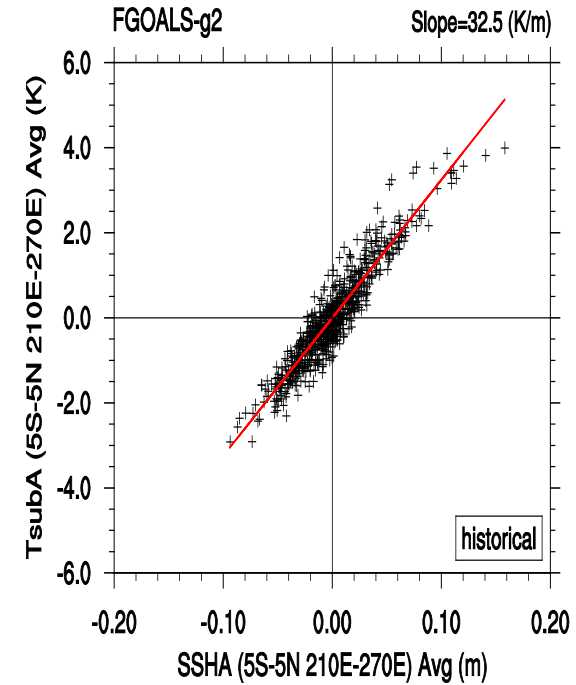
Three feedback processes



$$R(\tau'_x, T')$$

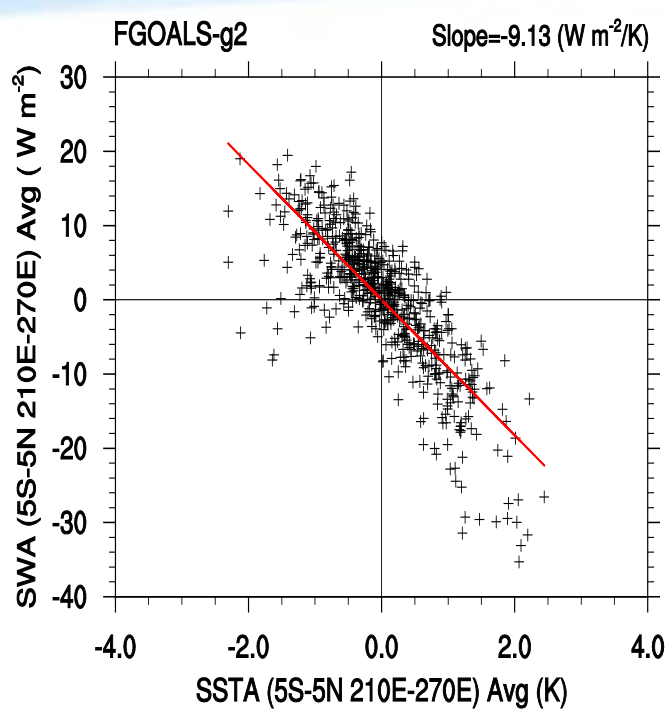


$$R(D', \tau'_x)$$

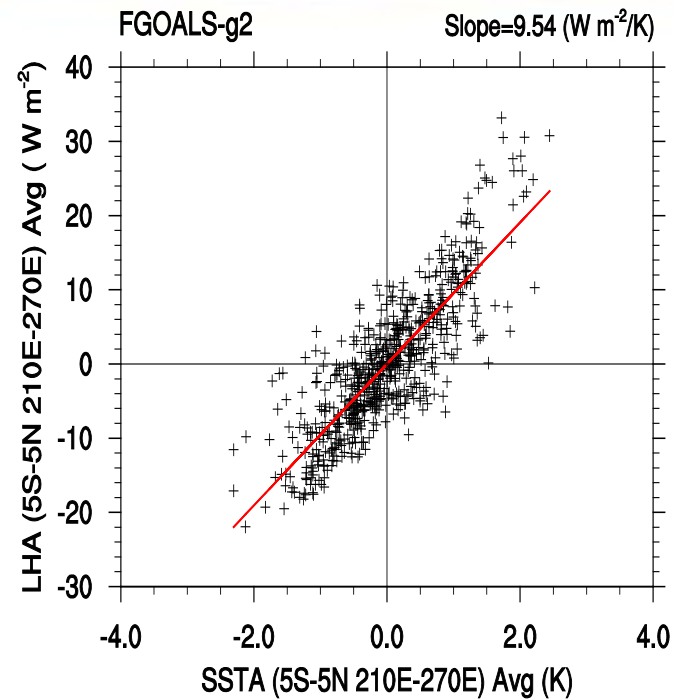


$$R(T'_e, D')$$

Thermodynamic-related feedbacks (SW feedback and LH feedback)



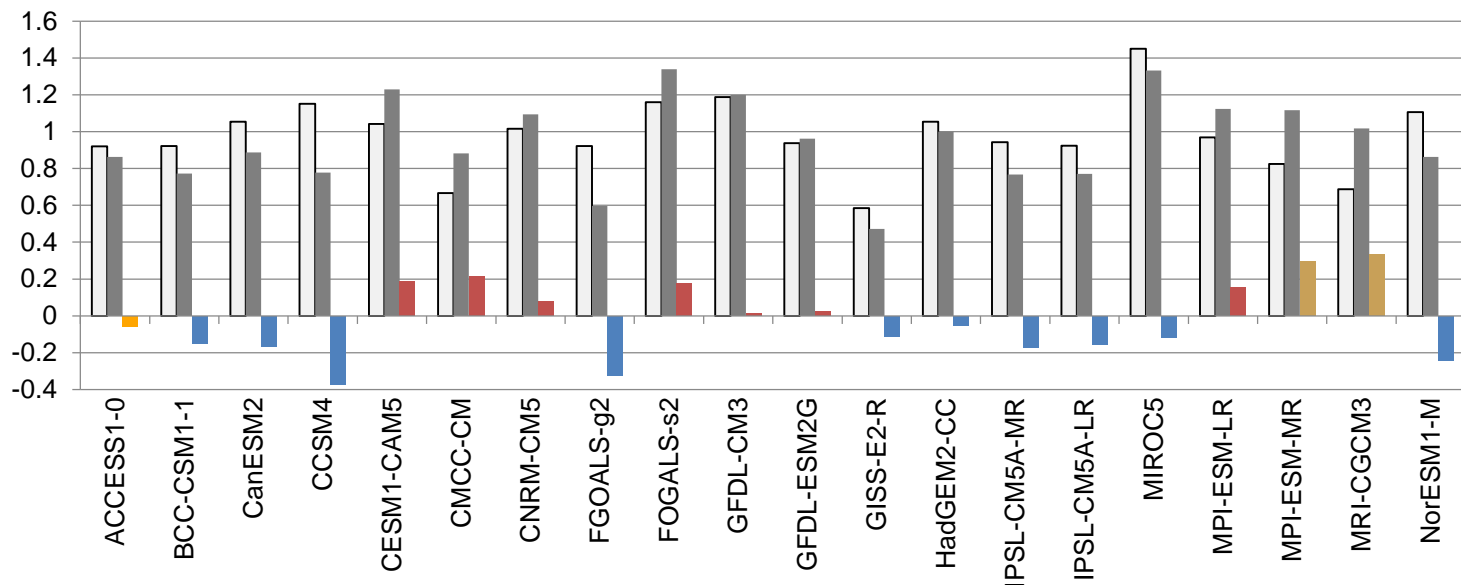
$$R(SW', T')$$



$$R(LH', T')$$

Example 2: Understand the cause of divergent projections of ENSO amplitude change under Global Warming in CMIP5 models

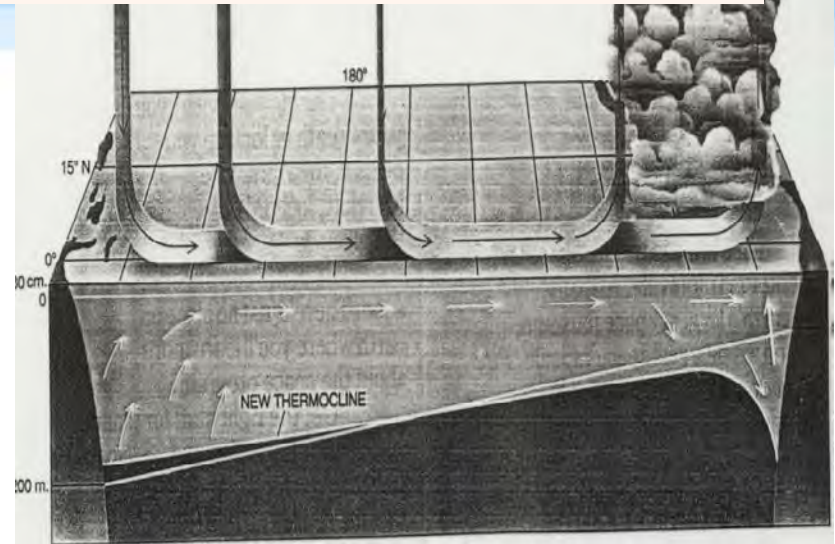
Nino3 SSTA Standard Deviation in PD, GW, GW-PD / $\text{GW} - \text{PD}$



ENSO development involves various positive feedbacks

$$\frac{\partial T'}{\partial t} \approx -u'T_x - w'T_z - \bar{w}T'_z$$

ZA Ekman TH

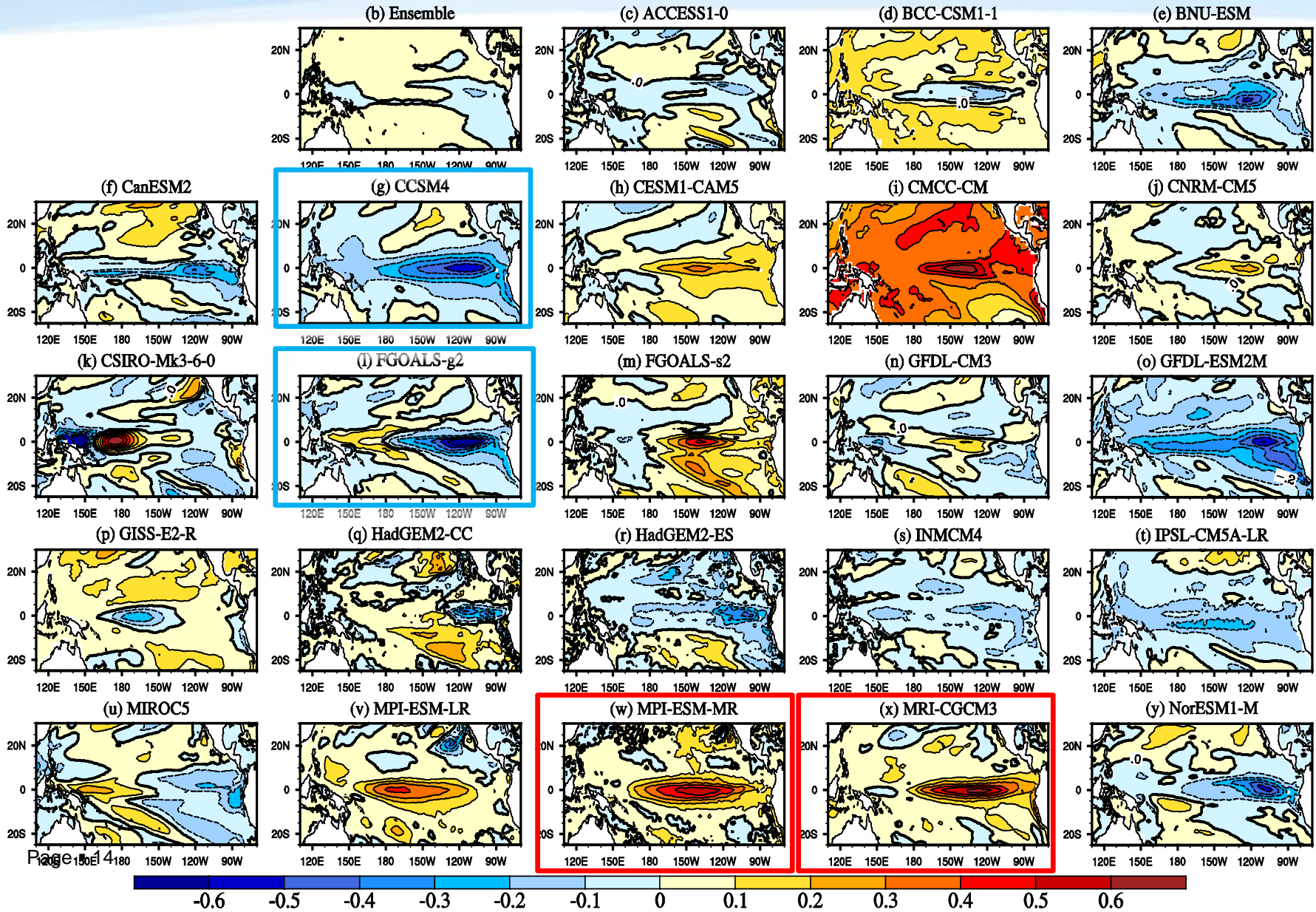


Science Question:

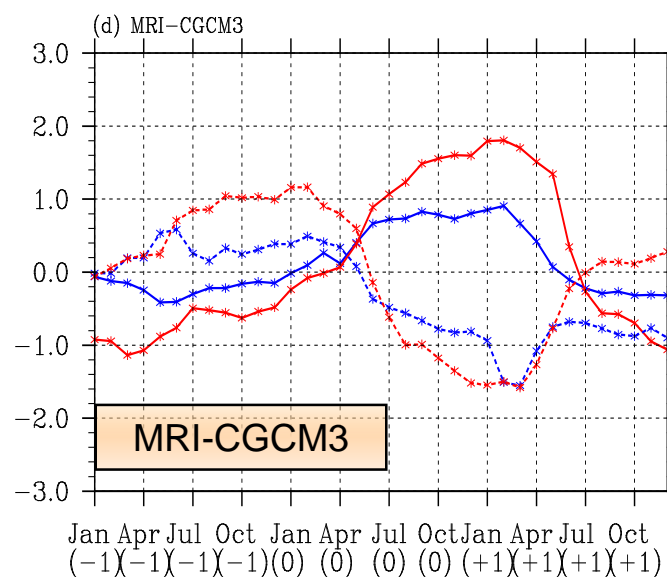
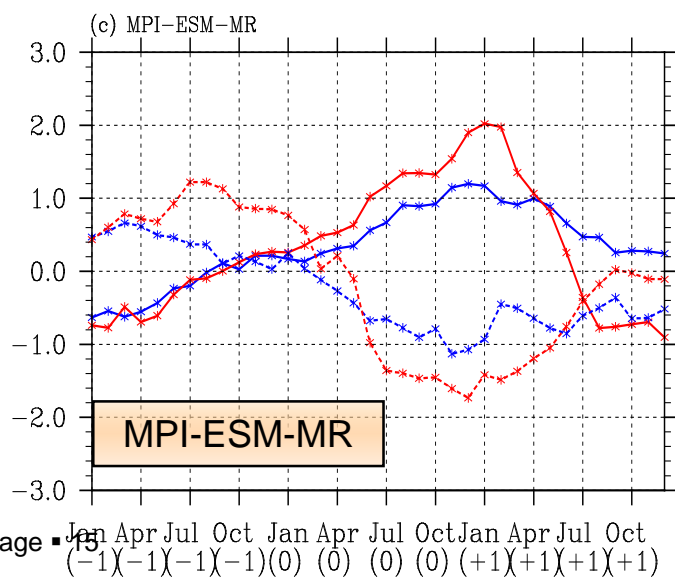
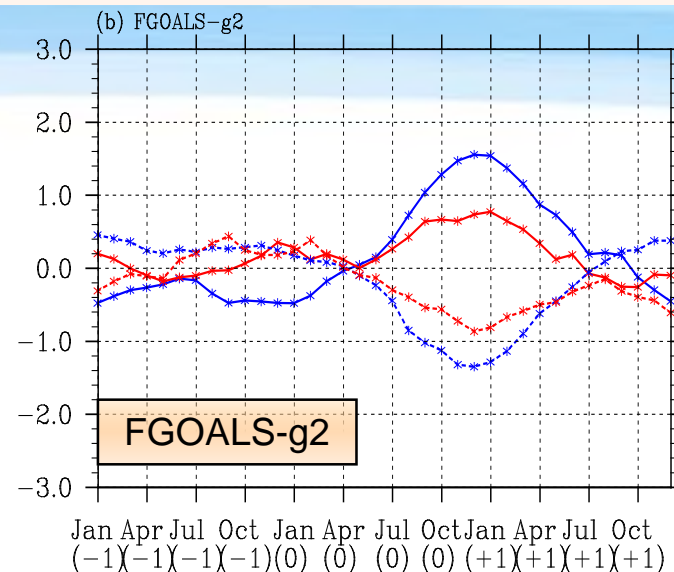
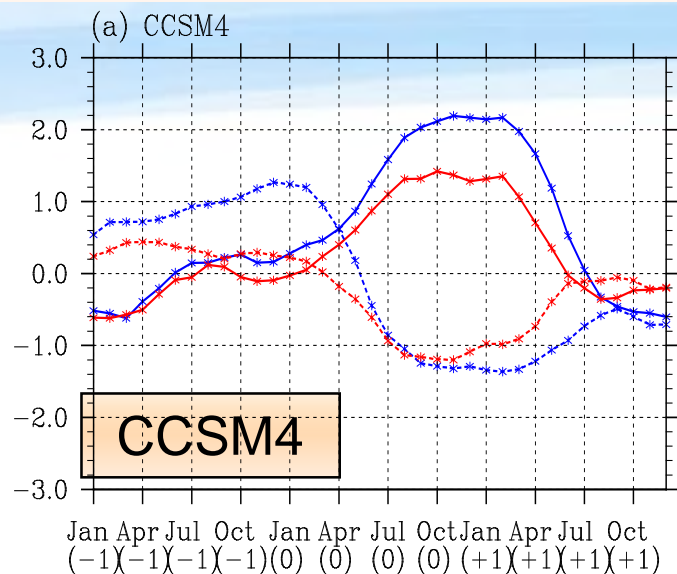
What feedback term is critical in causing divergent ENSO projections under GW within 20+ CMIP5 models?

Change of SSTA STD pattern: RCP85 (2051-2100) minus historical (1951-2000)

(SST has been de-trended)



Composite evolutions of El Nino and La Nina in 4 CGCMs



Mixed-layer Heat Budget Analysis

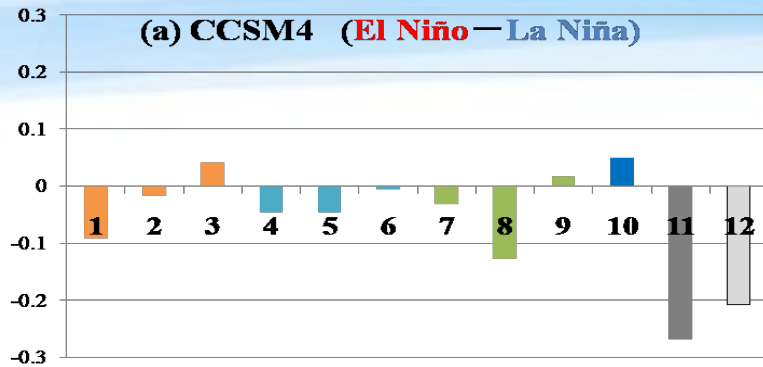
The mixed layer temperature tendency equation:

$$\frac{\partial T'}{\partial t} = \underbrace{-u' \frac{\partial \bar{T}}{\partial x}}_{(1)} \underbrace{-\bar{u} \frac{\partial T'}{\partial x}}_{(2)} \underbrace{-u' \frac{\partial T'}{\partial x}}_{(3)} \underbrace{-w' \frac{\partial \bar{T}}{\partial z}}_{(4)} \underbrace{-\bar{w} \frac{\partial T'}{\partial z}}_{(5)} \underbrace{-w' \frac{\partial T'}{\partial z}}_{(6)}$$

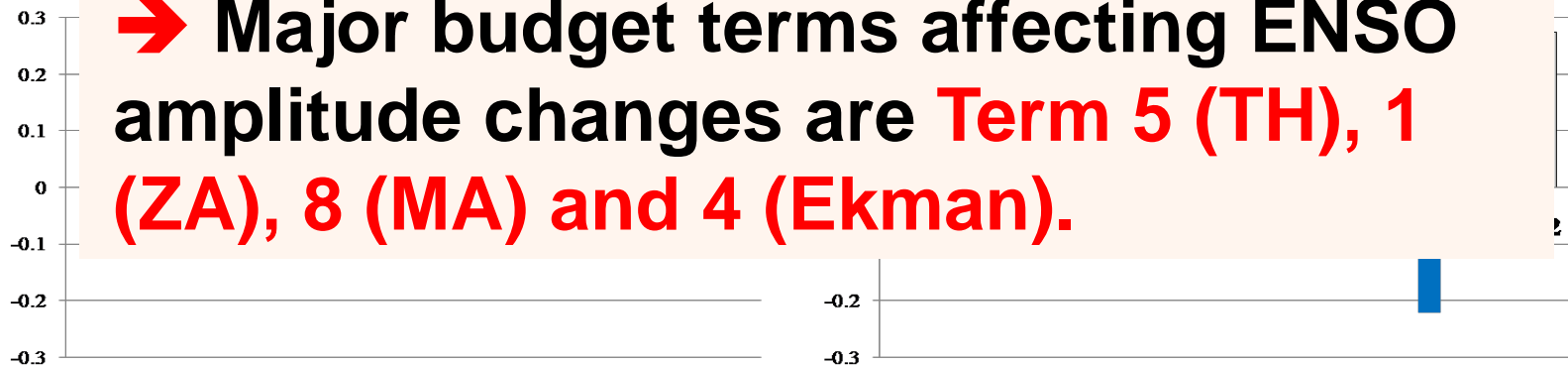
$$\underbrace{-v' \frac{\partial \bar{T}}{\partial y}}_{(7)} \underbrace{-\bar{v} \frac{\partial T'}{\partial y}}_{(8)} \underbrace{-v' \frac{\partial T'}{\partial y}}_{(9)} + \underbrace{\frac{Q'}{\rho C_p H}}_{(10)} + R$$

We examine the MLT tendency during **ENSO developing phase** (Apr-Nov[year 0]) for each of the CGCMs.

Composite MLT Budget Terms (GW minus PD)



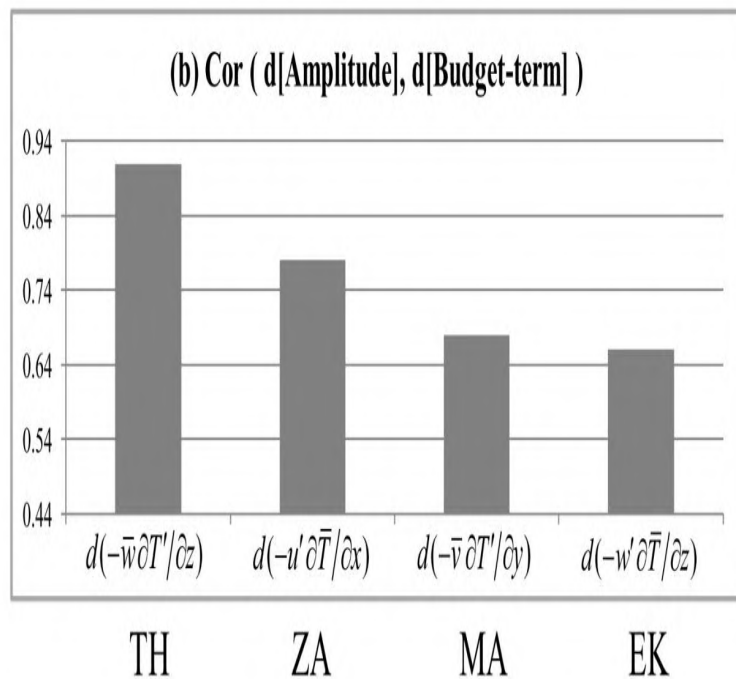
➔ Major budget terms affecting ENSO amplitude changes are **Term 5 (TH)**, **1 (ZA)**, **8 (MA)** and **4 (Ekman)**.



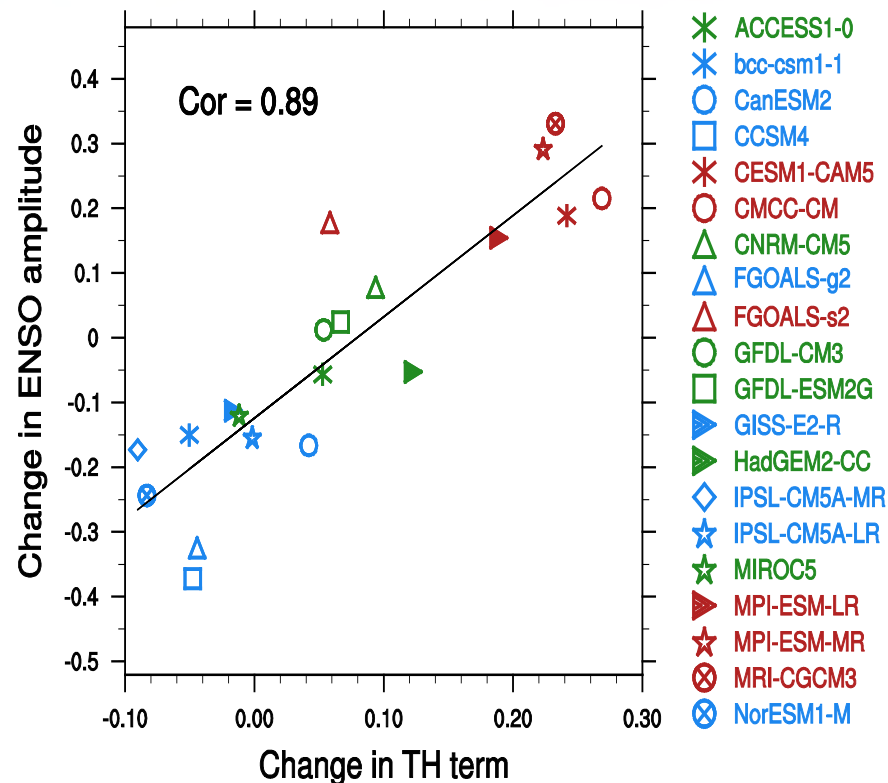
Term 1	Term 2	Term 3	Term 4	Term 5	Term 6	Term 7	Term 8	Term 9	Term 10	Term 11	Term 12
0.41	0.01	-0.10	0.22	0.54	0.01	0.01	0.32	-0.06	-0.5	0.86	0.88

- (1) $d(-u' \partial \bar{T} / \partial x)$ (2) $d(-\bar{u} \partial T' / \partial x)$ (3) $d(-u' \partial T' / \partial x)$ (4) $d(-w' \partial \bar{T} / \partial z)$ (5) $d(-\bar{w} \partial T' / \partial z)$ (6) $d(-w' \partial T' / \partial z)$
 (7) $d(-v' \partial \bar{T} / \partial y)$ (8) $d(-\bar{v} \partial T' / \partial y)$ (9) $d(-v' \partial T' / \partial y)$ (10) $d(Q' / \rho C_p H)$ (11) $d(\text{Adv} + Q_{\text{net}})$ (12) $d(\partial T' / \partial t)$

Correlation between ENSO Amplitude Change and MLT Budget Terms among 20 CMIP5 models



95% confidence level: 0.44



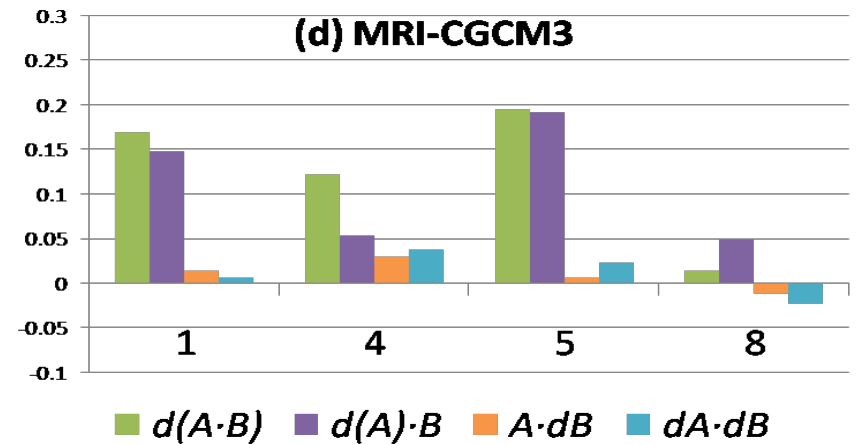
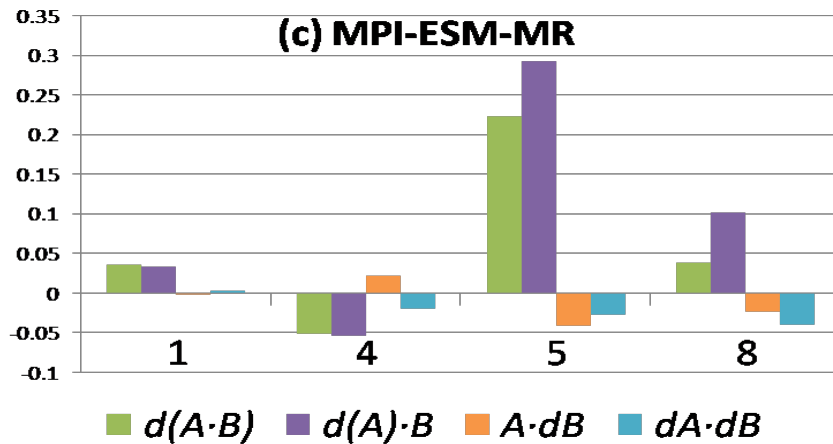
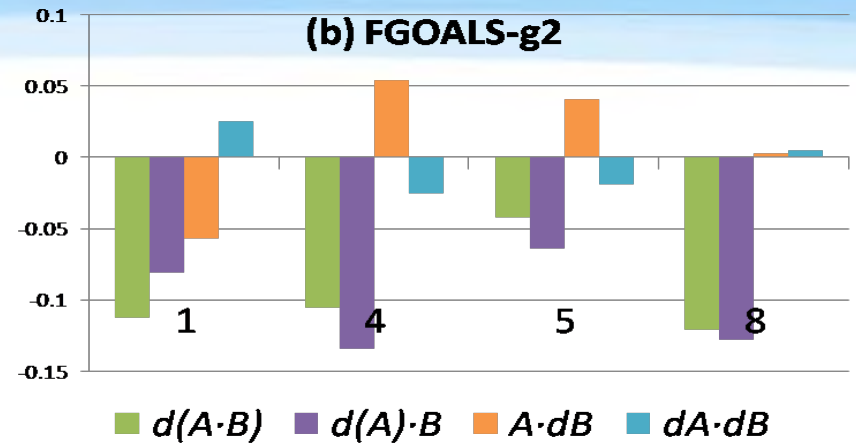
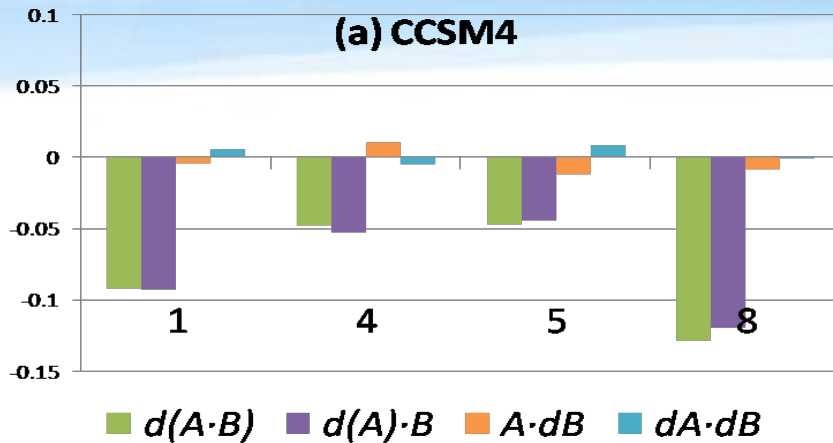
→ TH and ZA feedbacks are major drivers for the divergent ENSO amplitude changes.

Science Question 2:

The changes of all feedbacks mentioned above involve both the changes of the **mean state** and **perturbation**. Which change, **mean state or perturbation change**, is critical in determining the MLT tendency change?

$$\begin{aligned} \frac{\partial T'}{\partial t} &= -u' \frac{\partial \bar{T}}{\partial x} - \bar{u} \frac{\partial T'}{\partial x} - u' \frac{\partial T'}{\partial x} - w' \frac{\partial \bar{T}}{\partial z} - \bar{w} \frac{\partial T'}{\partial z} - w' \frac{\partial T'}{\partial z} \\ &\quad (1) \quad (2) \quad (3) \quad (4) \quad (5) \quad (6) \\ &\quad -v' \frac{\partial \bar{T}}{\partial y} - \bar{v} \frac{\partial T'}{\partial y} - v' \frac{\partial T'}{\partial y} + \frac{Q'}{\rho C_p H} + R \\ &\quad (7) \quad (8) \quad (9) \quad (10) \end{aligned}$$

Relative Role of **Perturbation** vs. **Mean State** Changes



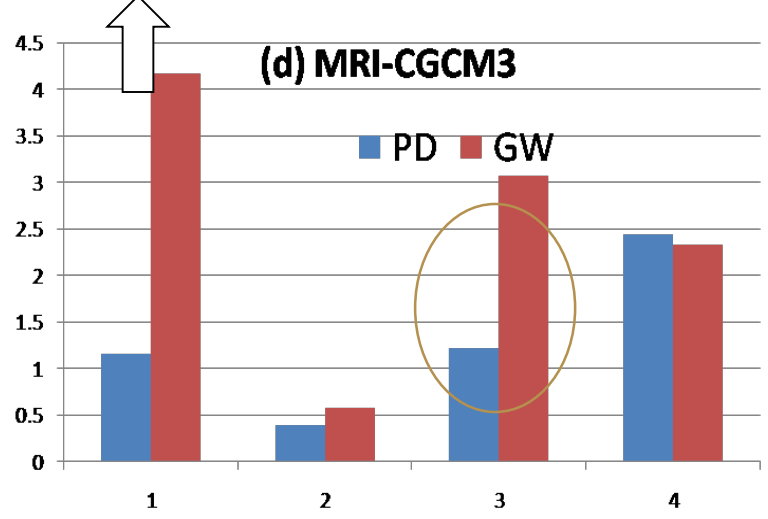
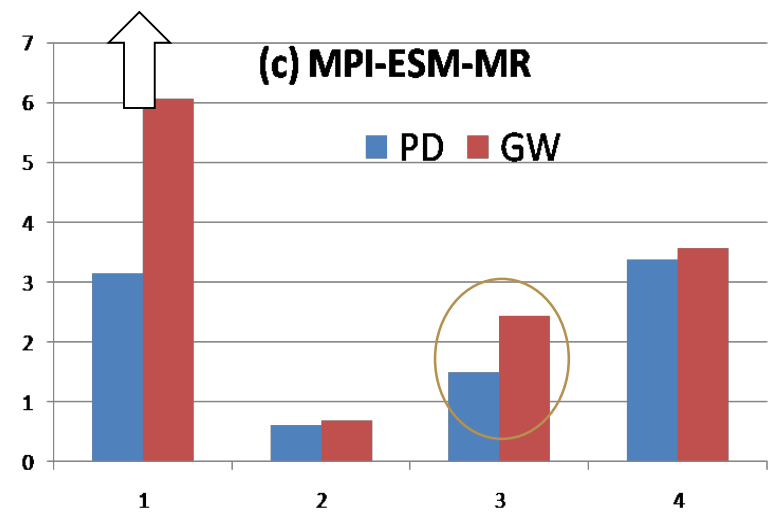
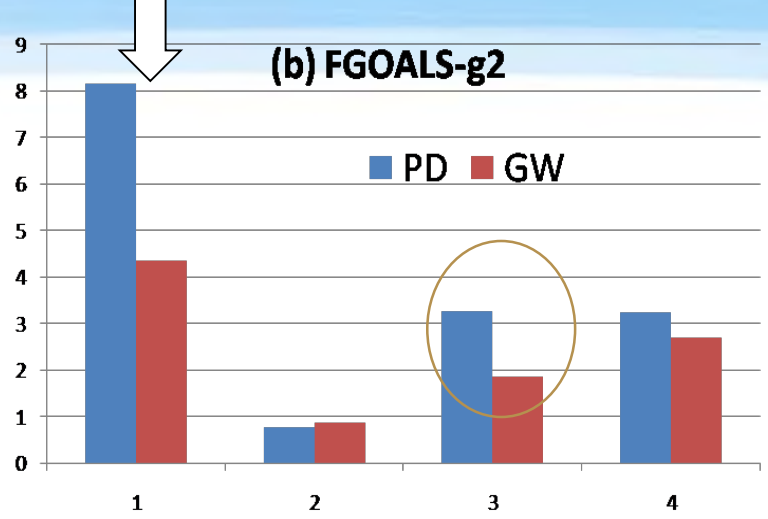
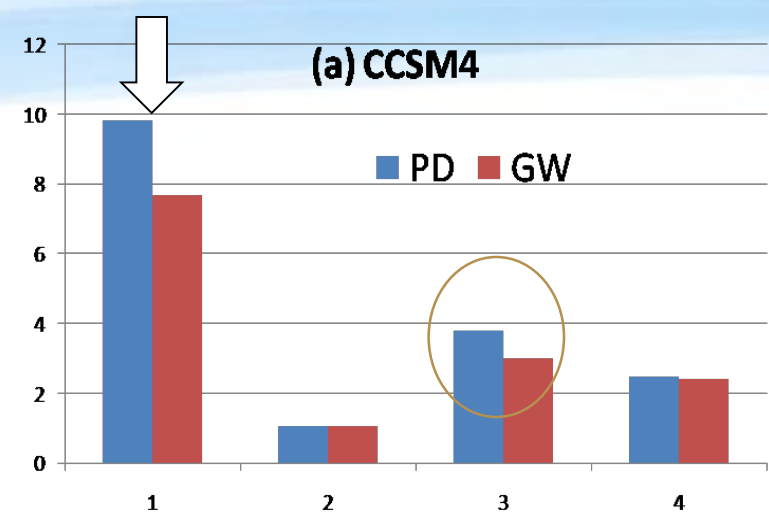
➔ The **change of perturbation** is critical for the diverged ENSO amplitude projections. This indicates that the **direct** impact of the mean state change is negligible.

Bjerknes TH Feedback (Liu, Li et al. 2012, J. Climate):

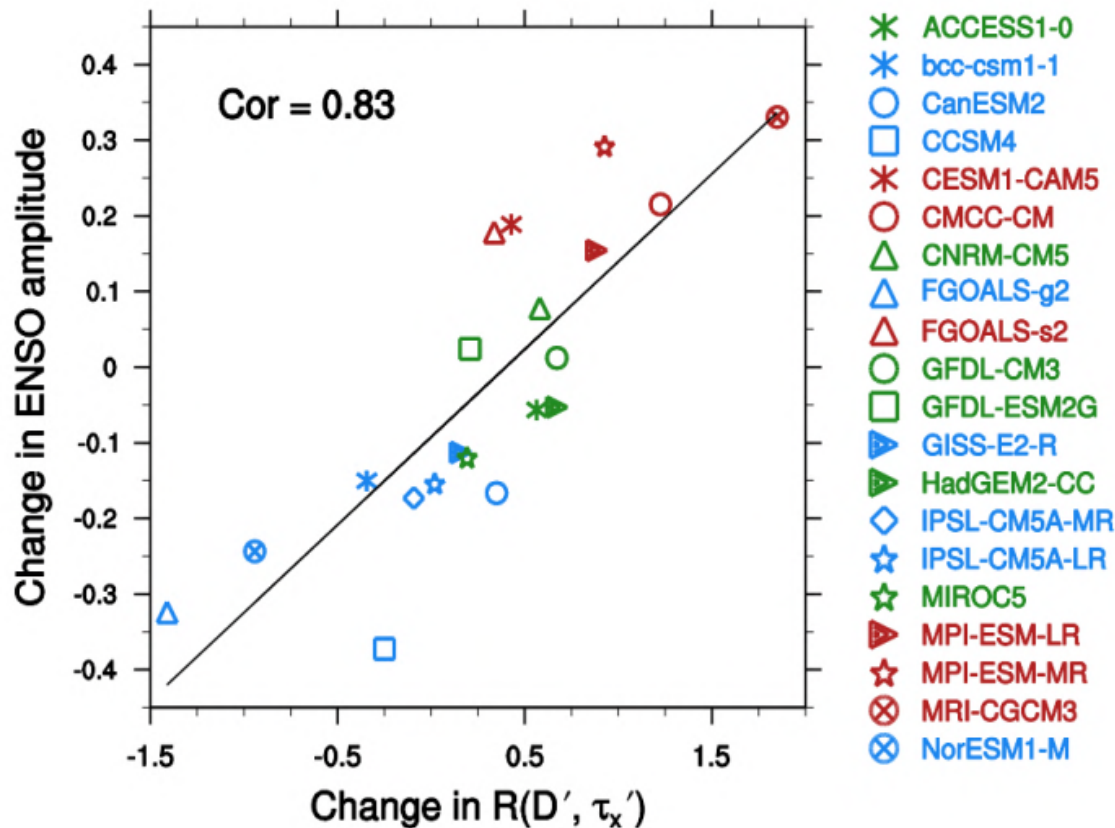
Growth rate:
$$\sigma = \frac{\bar{w}}{H} R(\tau_x', T') R(D', \tau_x') R(T_e', D')$$

Science Question 3:

The Bjerknes TH feedback involves 1) **how the atmospheric wind responds to unit SSTA forcing**, 2) **how strong the ocean TH responds to unit wind stress forcing**, and 3) **how strong the subsurface temperature responds to unit TH change**. **Which feedback coefficient change is critical in determining the ENSO amplitude change?**



ENSO Amplitude Change vs. $R(D', \tau_x')$ in 20 CMIP5 models



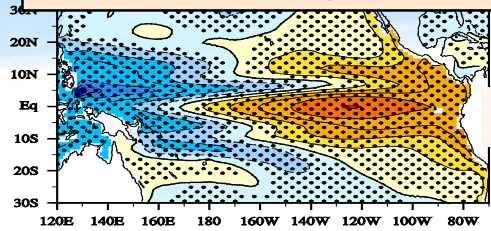
ST: 7 ENSO strengthened model group (red);

WK: 7 ENSO weakened model group (blue).

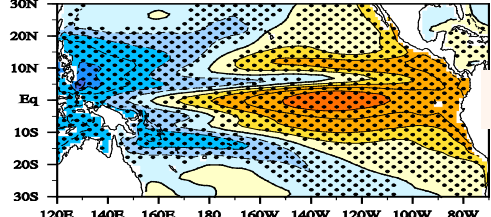
A further analysis shows that in **ZA feedback**, u' is primarily determined by **geostrophic current** anomaly, which is also related to **the TH anomaly**. Thus, **the distinctive changes of thermocline response to the wind forcing** hold a key for explaining the ENSO amplitude change under GW.

Composite Thermocline Response to τ_{aux} ' and ENSO Meridional Structure Change

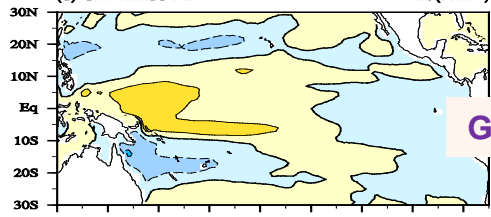
ENSO Weakening Models



(b) GW $\text{m}/(\text{N m}^2)$

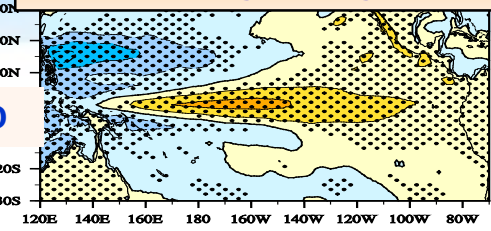


(c) GW minus PD $\text{m}/(\text{N m}^2)$

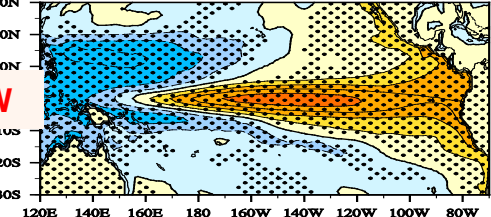


(d) GW minus PD $\text{m}/(\text{N m}^2)$

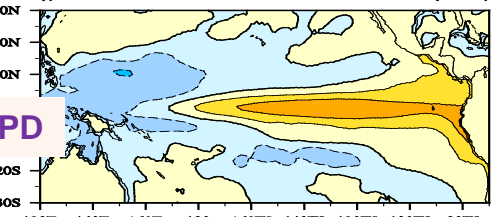
ENSO Strengthening Models



(f) GW $\text{m}/(\text{N m}^2)$



(h) GW minus PD $\text{m}/(\text{N m}^2)$



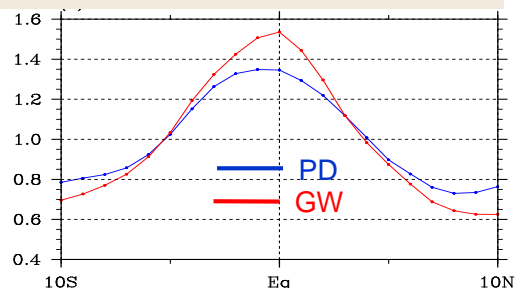
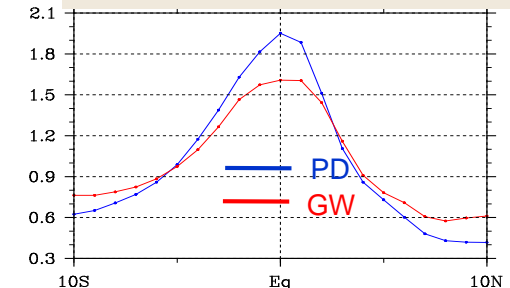
(j) GW minus PD $\text{m}/(\text{N m}^2)$

PD

GW

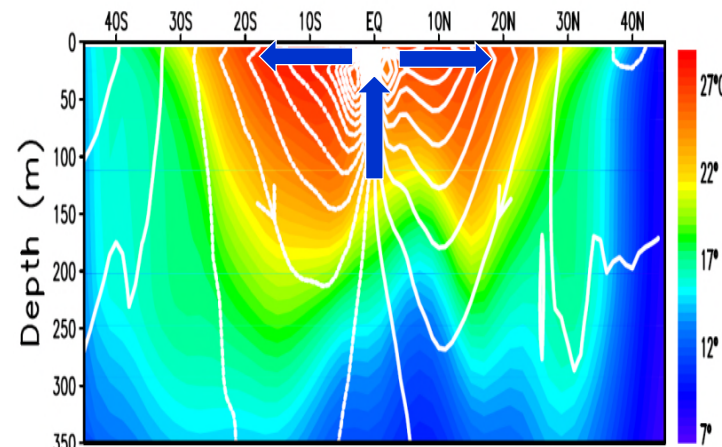
GW - PD

ENSO Meridional Structure in PD and GW State



What controls the ENSO meridional structure?

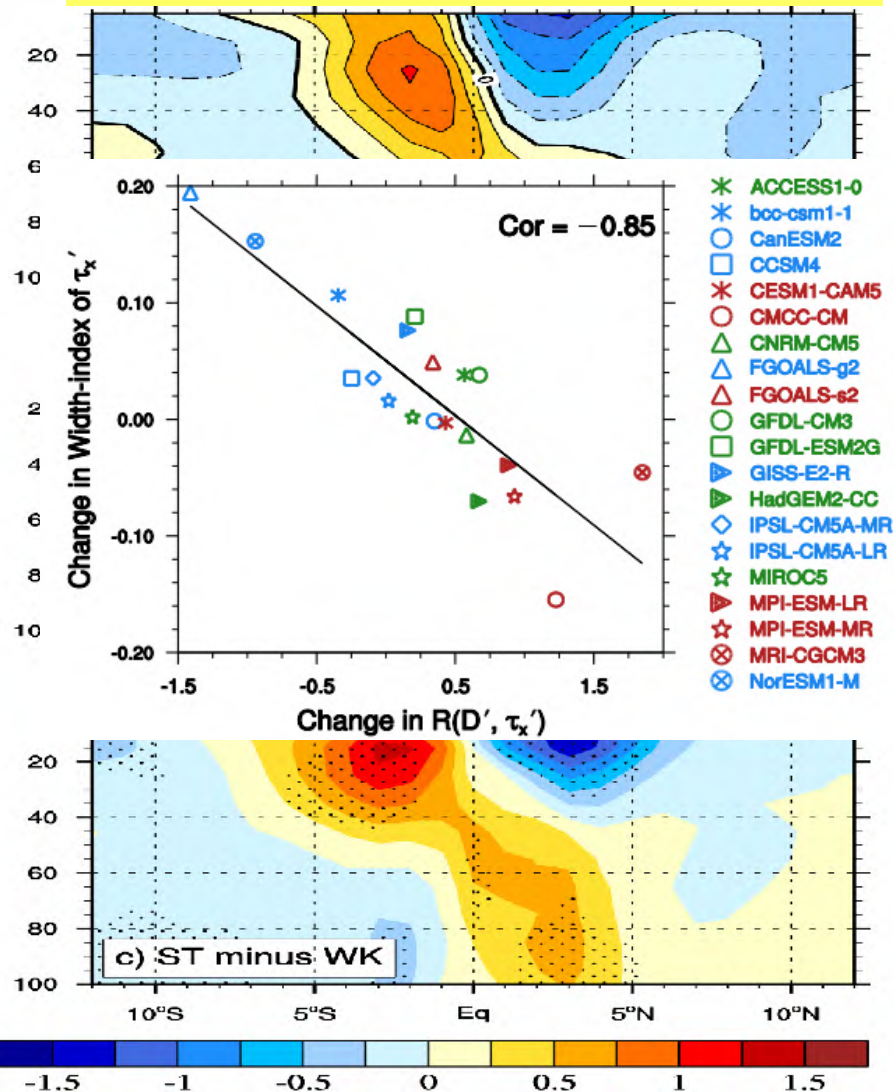
→ Pacific Subtropical Cell (STC)



Climatological Subtropical Cell (STC)
(from Nonaka et al., 2002)

A Robust Relationship between ENSO and STC Change

Meridional Ocean Current Change



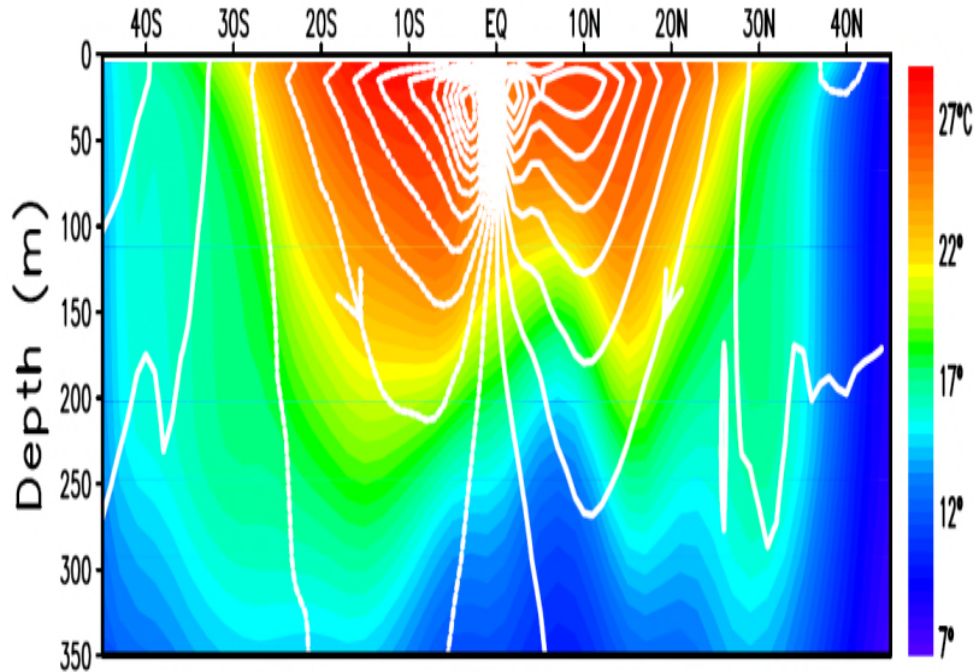
Strengthened
ENSO

Enhanced
 $R(D', \tau'_x)$

Steeper ENSO
Meridional
Structure

Weakened STC

Step 2: Project how Pacific climatological STC would change under global warming



What controls the strength of climatological mean STC ?

➔ Strength of trade winds / SST gradients

An analytical model to understand SST change under global warming

$$\rho C_p h \frac{\partial T}{\partial t} = Q_{net} + D_{ocean}$$

Ocean mixed layer heat budget

D_{ocean} : Ocean dynamical effect

Quasi-equilibrium state assumption: Climate states are in statistically equilibrium in both PD and GW, respectively. For annual average, time tendency term can be dropped and the difference between GW and PD ($\delta = \text{GW} - \text{PD}$) satisfies:

$$\delta Q_{net} + \delta D_{ocean} = 0$$

$$\delta Q_{sw} + \delta Q_{lw}^{down} - \delta Q_{lw}^{up} - \delta Q_{lh} - \delta Q_{sh} + \delta D_{ocean} = 0$$

$$\delta Q_{sw} + \delta Q_{lw}^{down} - 4\sigma \overline{T_s}^3 \delta T_s - \delta Q_{lh}^{atmos} - \gamma_1 \overline{Q_{lh}} \delta T_s - \delta Q_{sh}^{atmos} - \gamma_2 \overline{V} \delta T_s + \delta D_{ocean} = 0$$

$$\delta T_s = \frac{\delta Q_{sw} + \delta Q_{lw}^{down} - \delta Q_{lh}^{atmos} - \delta Q_{sh}^{atmos} + \delta D_{ocean}}{\gamma_1 \overline{Q_{lh}} + 4\sigma \overline{T_s}^3 + \gamma_2 \overline{V}}$$

Analytical model to understand SST change under global warming (Con.)

To the first order, assume that circulation/cloud change is too small to affect the SST change.

$$\delta T_s = \frac{\delta Q_{sw} + \delta Q_{lw}^{down} - \delta Q_{lh}^{atmos} - \delta Q_{sh}^{atmos} + \delta D_{ocean}}{\gamma_1 \overline{Q_{lh}} + 4\sigma \overline{T_s}^3 + \gamma_2 \overline{V}}$$

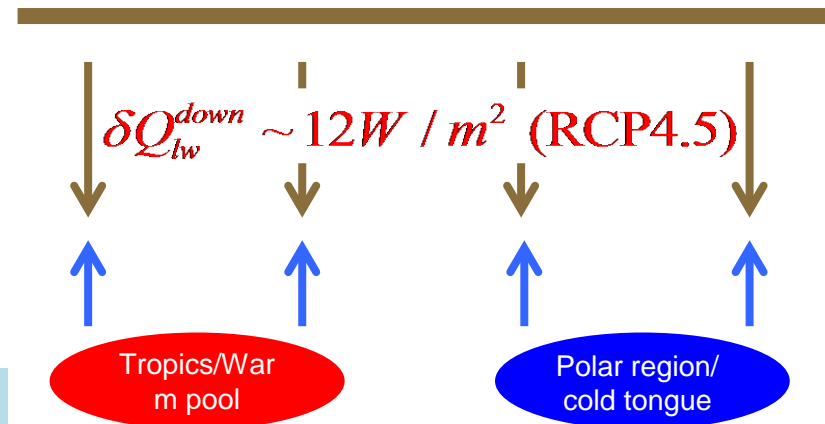
Zhang and Li 2014 J. Climate

$$\delta T_s = \frac{\text{Uniform } \delta Q_{lw}^{down}}{\gamma_1 \overline{Q_{lh}} + 4\sigma \overline{T_s}^3 + \gamma_2 \overline{V}}$$

$$\delta Q_{lw}^{down} = (\gamma_1 \overline{Q_{lh}} + 4\sigma \overline{T_s}^3 + \gamma_2 \overline{V}) * \delta T_s$$

$$\delta Q_{lw}^{down} = 4\sigma \overline{T_s}^3 * \delta T_s \sim \delta T_s = \frac{\delta Q_{lw}^{down}}{4\sigma \overline{T_s}^3}$$

Longwave radiative – evaporative damping mechanism



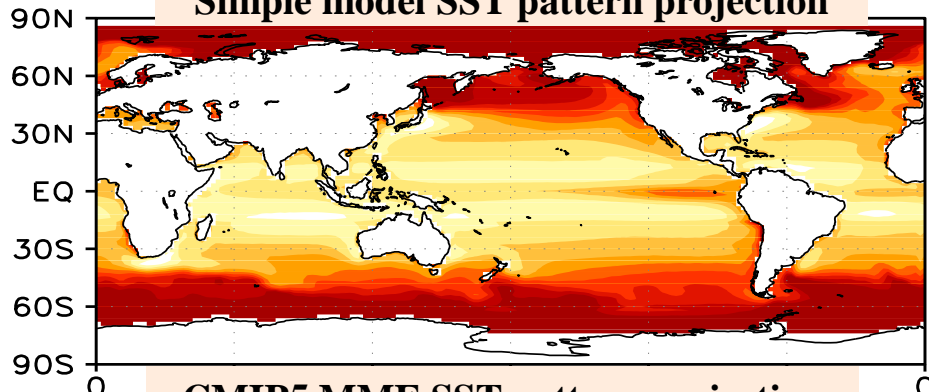
An analytical model for mean SST change under global warming

$$\delta T_s = \frac{\cancel{\delta Q_{sw}} + \delta Q_{lw}^{down} - \delta Q_{lh}^{atmos} - \delta Q_{sh}^{atmos} + \cancel{\delta D_{ocean}}}{\gamma_1 \overline{Q_{lh}} + 4\sigma \overline{T_s}^3 + \gamma_2 \overline{V}}$$

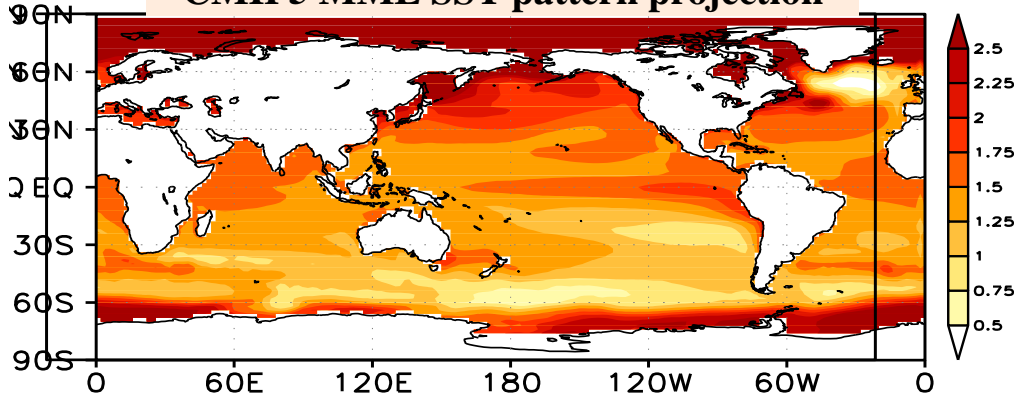
Zhang and Li 2014 J. Climate

To the first order, assume that circulation/ cloud change is too small to affect the SST change.

Simple model SST pattern projection



CMIP5 MME SST pattern projection

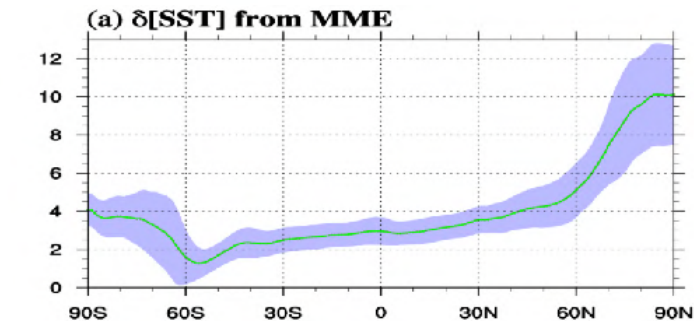


Pattern correlation coefficient: 0.7

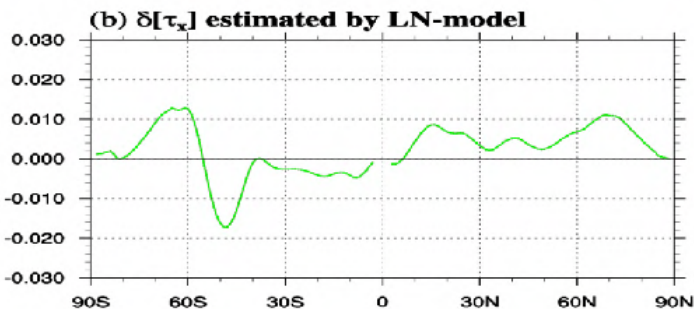
The simple model is able to capture

- Polar amplification;
- El Nino like warming;
- Greater warming at the equator than in subtropics.

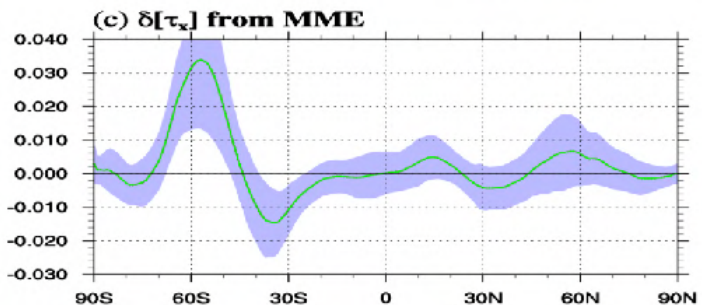
Given the robust zonal mean SST projection, how would zonal wind and STC change under GW?



← 20+ CMIP5 model **ensemble mean projection** of the **zonal mean SST change**



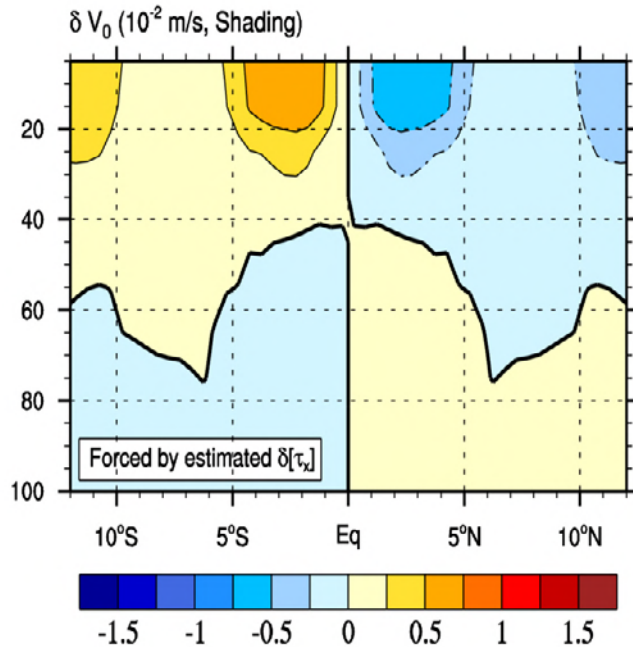
← Estimated zonal mean zonal wind stress change based on **Lindzen and Nigam (1987)** model



← CMIP5 MME projection of zonal mean zonal wind stress change.

Pattern correlation coefficient: 0.6 (30S-30N)

OGCM simulations forced by the theoretically estimated zonal wind stress change



STC is weakened under GW!

The same conclusion is derived when forced by the CMIP5 MME derived wind stress change field.

Summary and Conclusion:

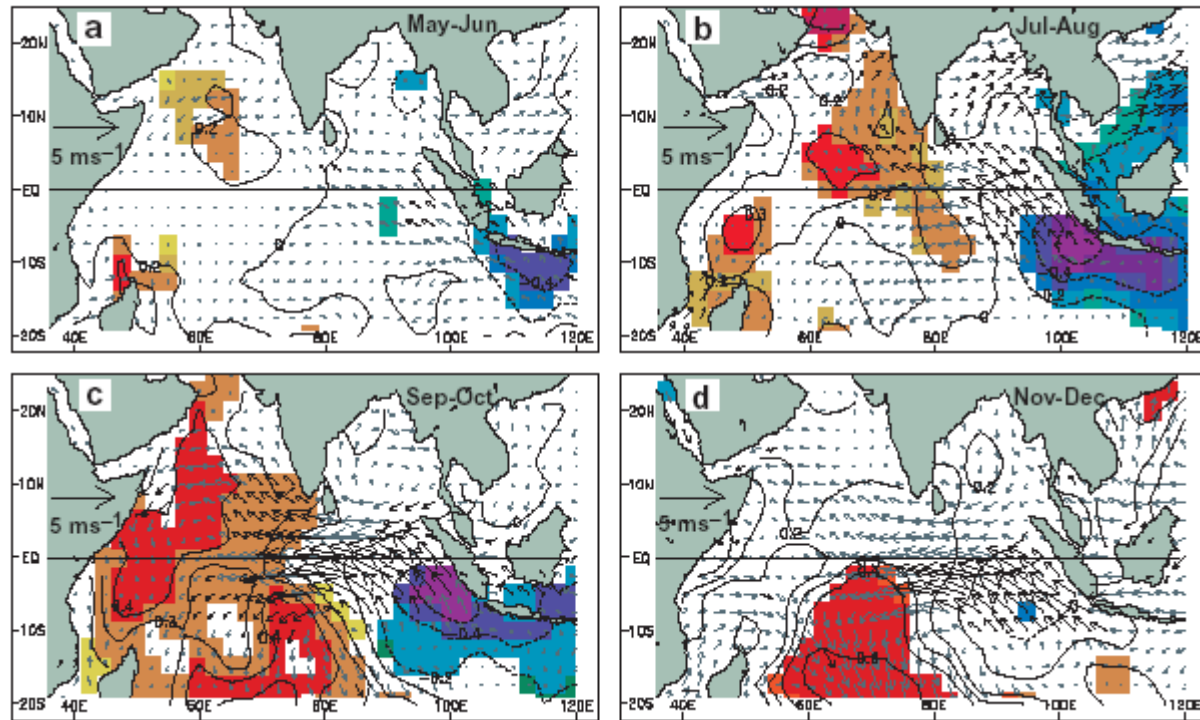
A two-step ENSO projection strategy was developed.

Step 1: ENSO – STC relationship

Step 2: Robust zonal mean SST projection → zonal mean zonal wind stress/STC change

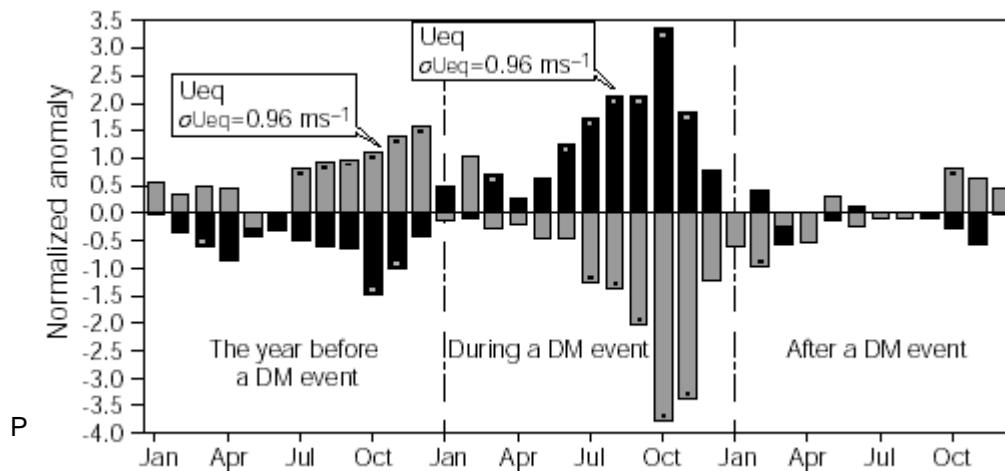
A weakened climatologic STC is projected in late 21C. This would favor a sharper ENSO meridional structure and thus an enhanced Bjerknes feedback and strengthened ENSO amplitude under GW.

Example 3: Diagnosis of the Indian Ocean Dipole



El Nino-like Variability in the Indian Ocean → Indian Ocean dipole (IOD)

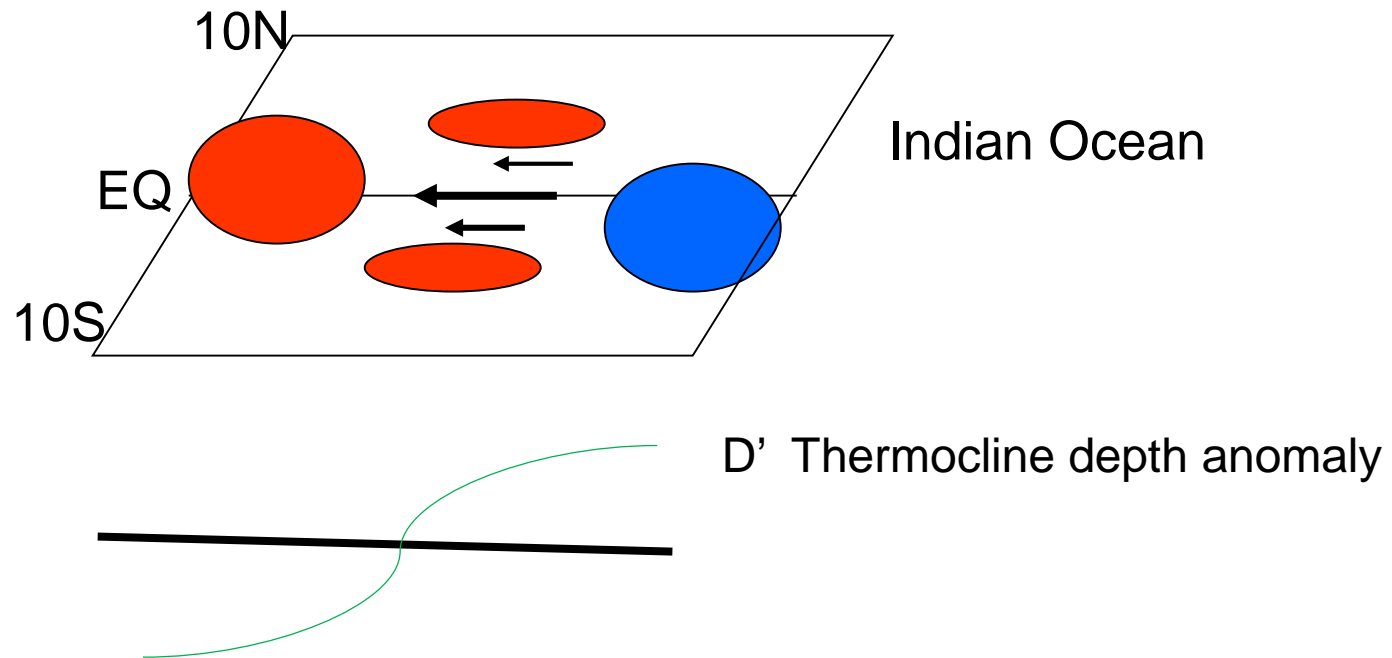
- 1) IOD is an air-sea coupled mode in Indian Ocean.
- 2) It involve Bjerknes' dynamic feedback.
- 3) Its peak phase occur in northern fall, different from El Nino which is mature in northern winter.
- 4) IOD has a great impact on Asian monsoon and East Asia climate.



(POSITIVE IOD PHASE :
1961,1967,1972,1982,1994,1997)

Saji et al. 1999

Schematic of Bjerknes dynamical feedback during IOD development

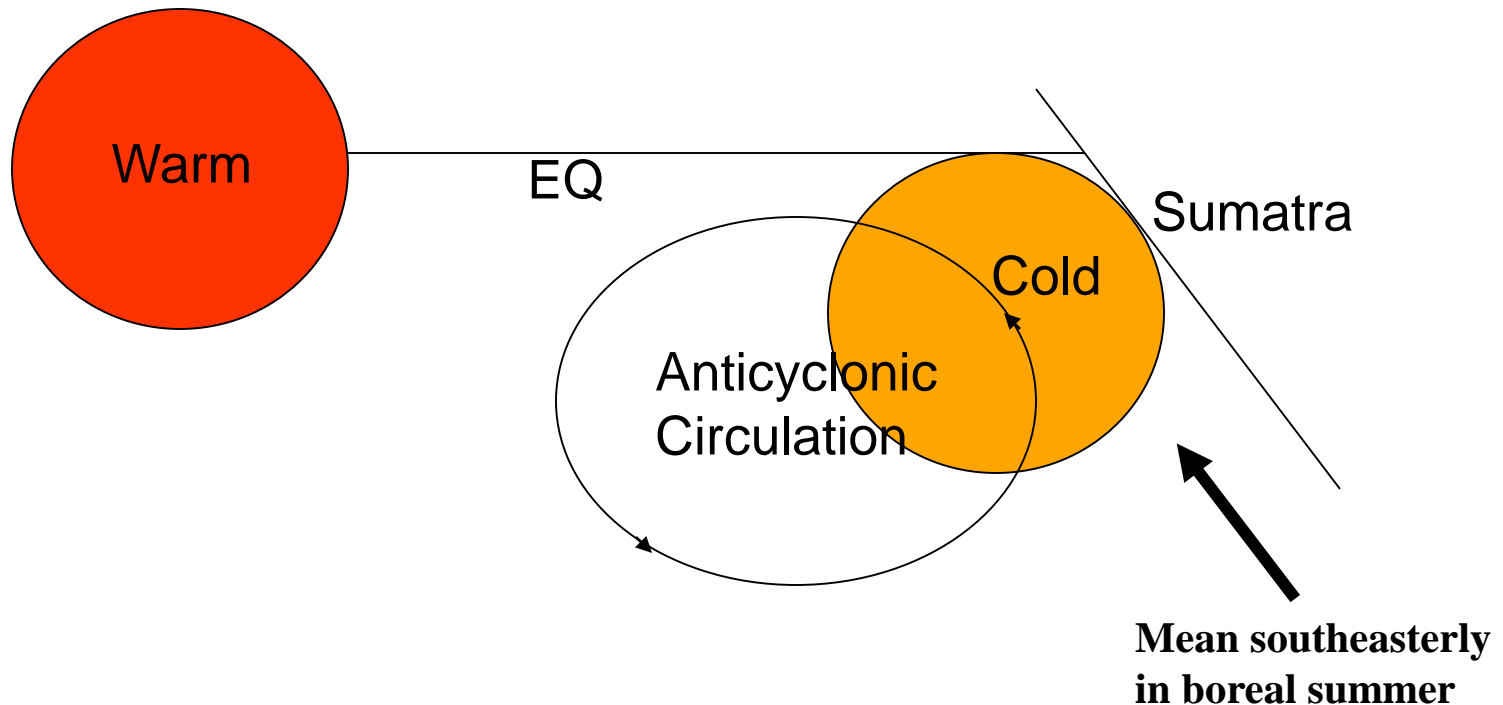


Steps to diagnose the Bjerknes dynamic feedback in a coupled model:

1. $R(u', T')$
2. $R(D', u')$
3. $R(Te', D')$

A Season-dependent Thermodynamic Air-Sea Feedback in the Southeast Indian Ocean

(Li et al. 2003, J. Atmos. Sci.)

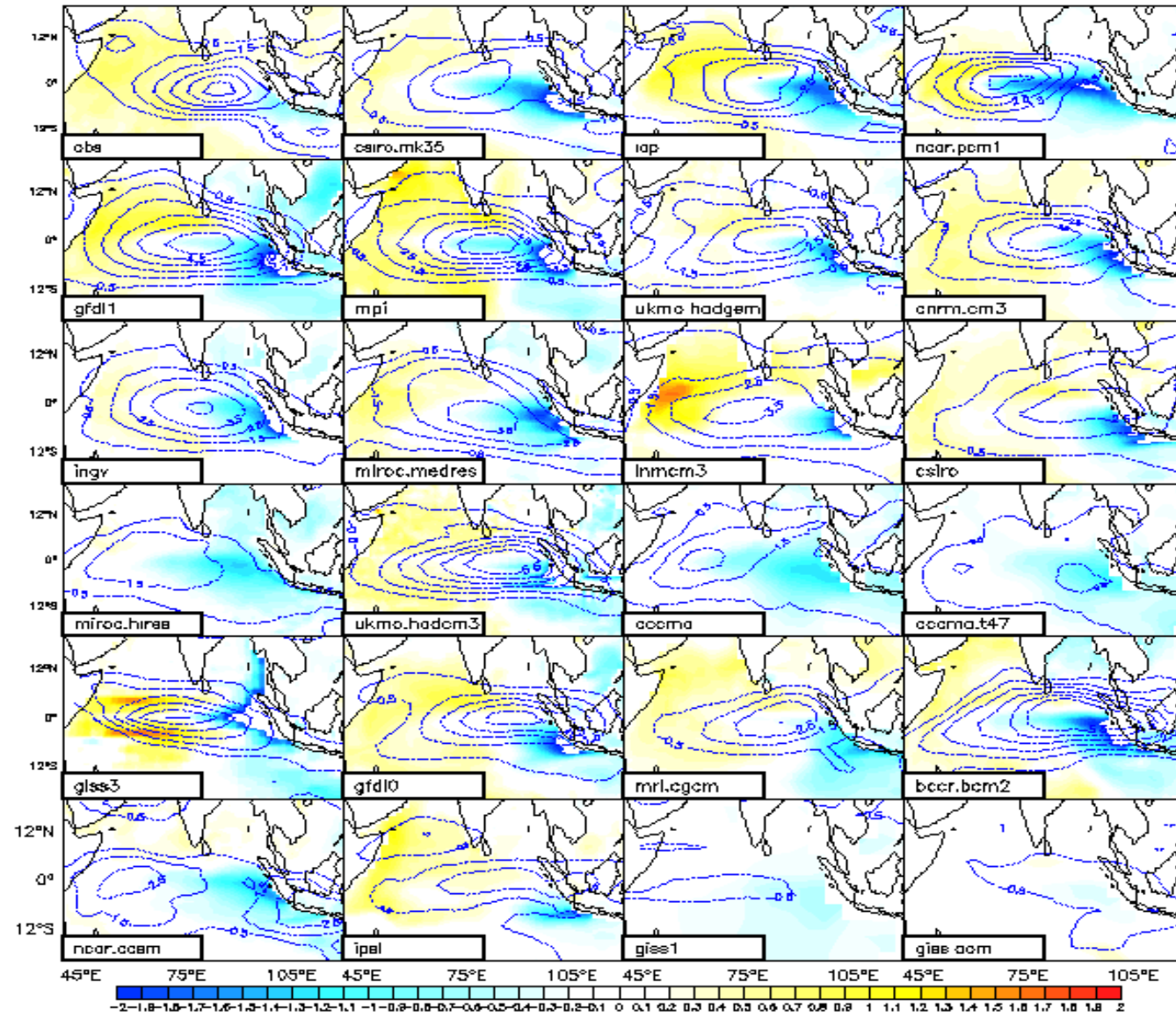


Boreal summer: **Positive** feedback

Boreal winter: **Negative** feedback

This explains why IOD peaks in boreal fall.

Composite SSTA (shading) and 850-hPa zonal wind anomaly fields in SON from the observation and 23 AR4 models



Rank the IOD simulation strength

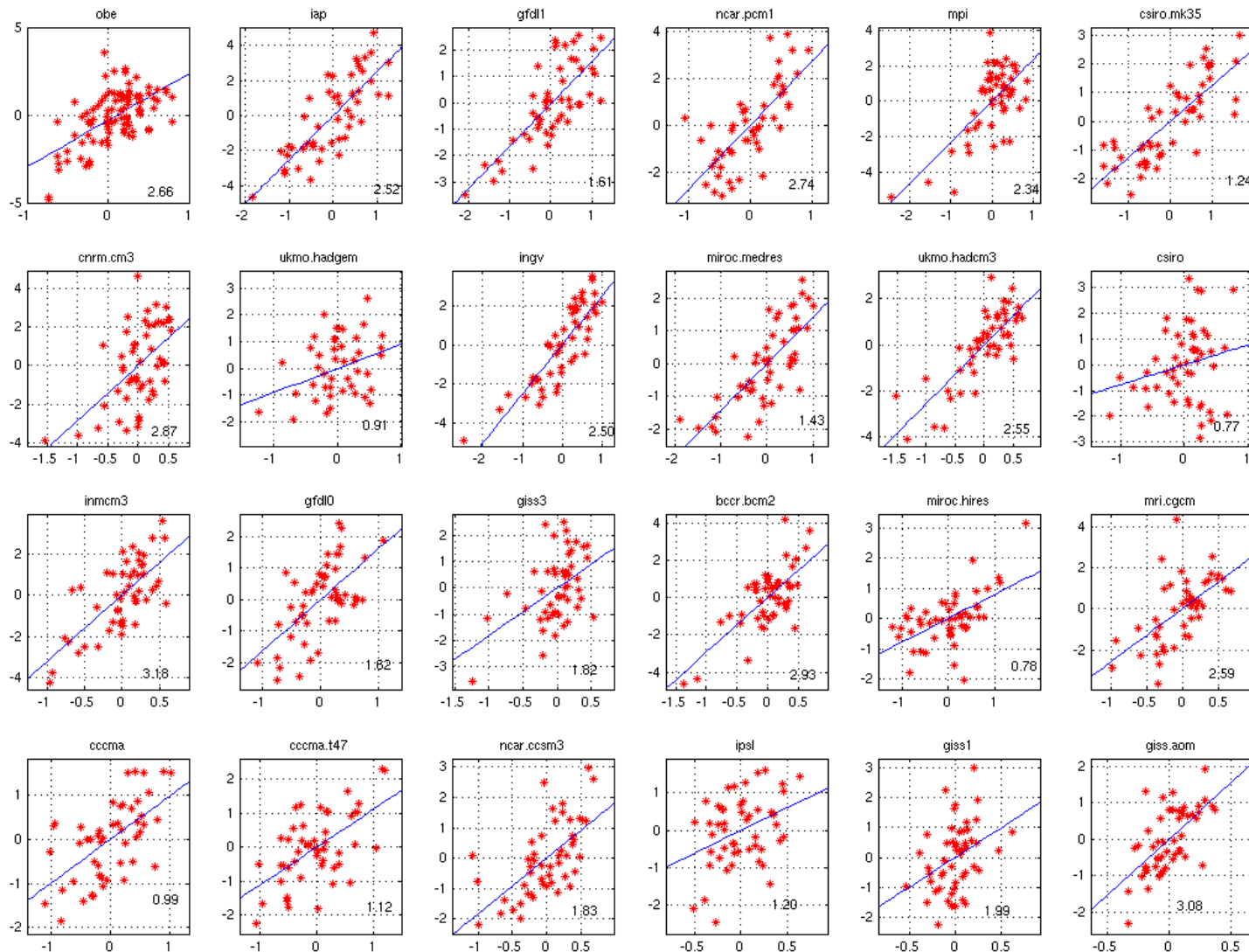
No.	ISI	DMI	EDMI	Model short name	CMIP model names
1	4.608	1.369	0.863	iap	FGOALS-g1.0
2	4.015	1.145	0.853	gfdl1	GFDL-CM2.1
3	3.841	1.242	0.874	ncar.pcm1	PCM
4	3.723	1.052	0.758	mpi	ECHAM5/MPI-OM
5	3.445	1.287	1.029	csiro.mk35	CSIRO-Mk3.5
6	2.904	1.014	0.707	cnrm.cm3	CNRM-CM3
7	2.687	0.787	0.644	ukmo.hadgem	UKMO-HadGEM1
8	2.455	0.886	0.722	ingv	INGV-SXG
9	2.417	0.920	0.687	miroc.medres	MIROC3.2(medres)
10	2.414	0.719	0.501	ukmo.hadcm3	UKMO-HadCM3
11	2.302	0.797	0.595	csiro	CSIRO-Mk3.0
12	2.203	0.963	0.525	inmcm3	INM-CM3.0
13	1.606	0.627	0.464	gfdl0	GFDL-CM2.0
14	1.393	0.631	0.481	giss3	GISS-EH
15	1.359	0.498	0.429	bccr.bcm2	BCCR-BCM2.0
16	1.323	0.638	0.609	miroc.hires	MIROC3.2(hires)
17	1.171	0.628	0.443	mri.cgcm	MRI-CGCM2.3.2
18	1.103	0.549	0.615	cccma	CGCM3.1(T63)
19	0.956	0.556	0.583	cccma.t47	CGCM3.1(T47)
20	0.700	0.424	0.424	ncar.cesm3	CCSM3
21	0.661	0.401	0.315	ipsl	IPSL-CM4
22	0.330	0.240	0.272	giss1	GISS-ER
23	0.158	0.201	0.207	giss.aom	GISS-AOM

S

M

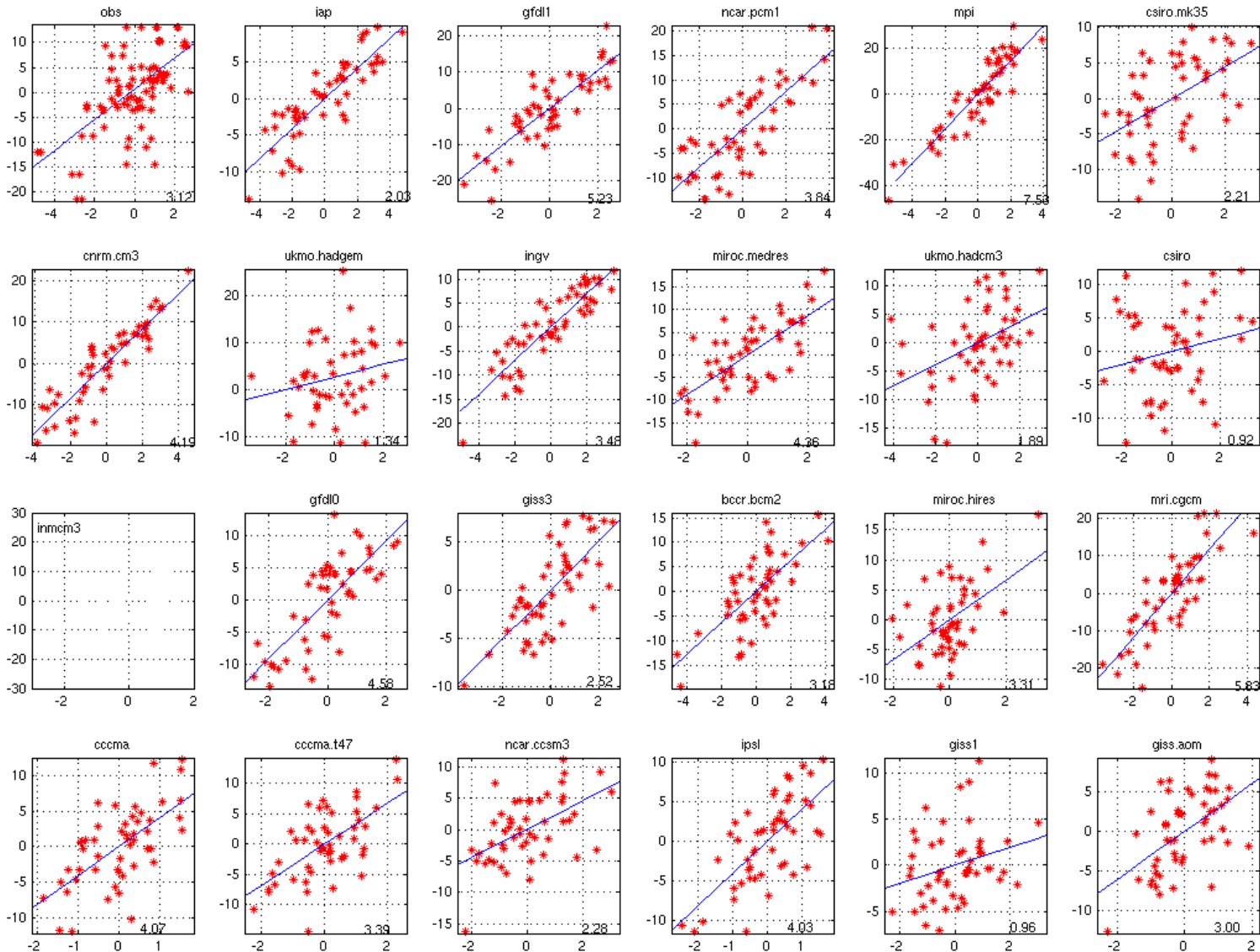
W

Diagnose the strength of atmospheric response to unit SSTA forcing, $R(u', T')$



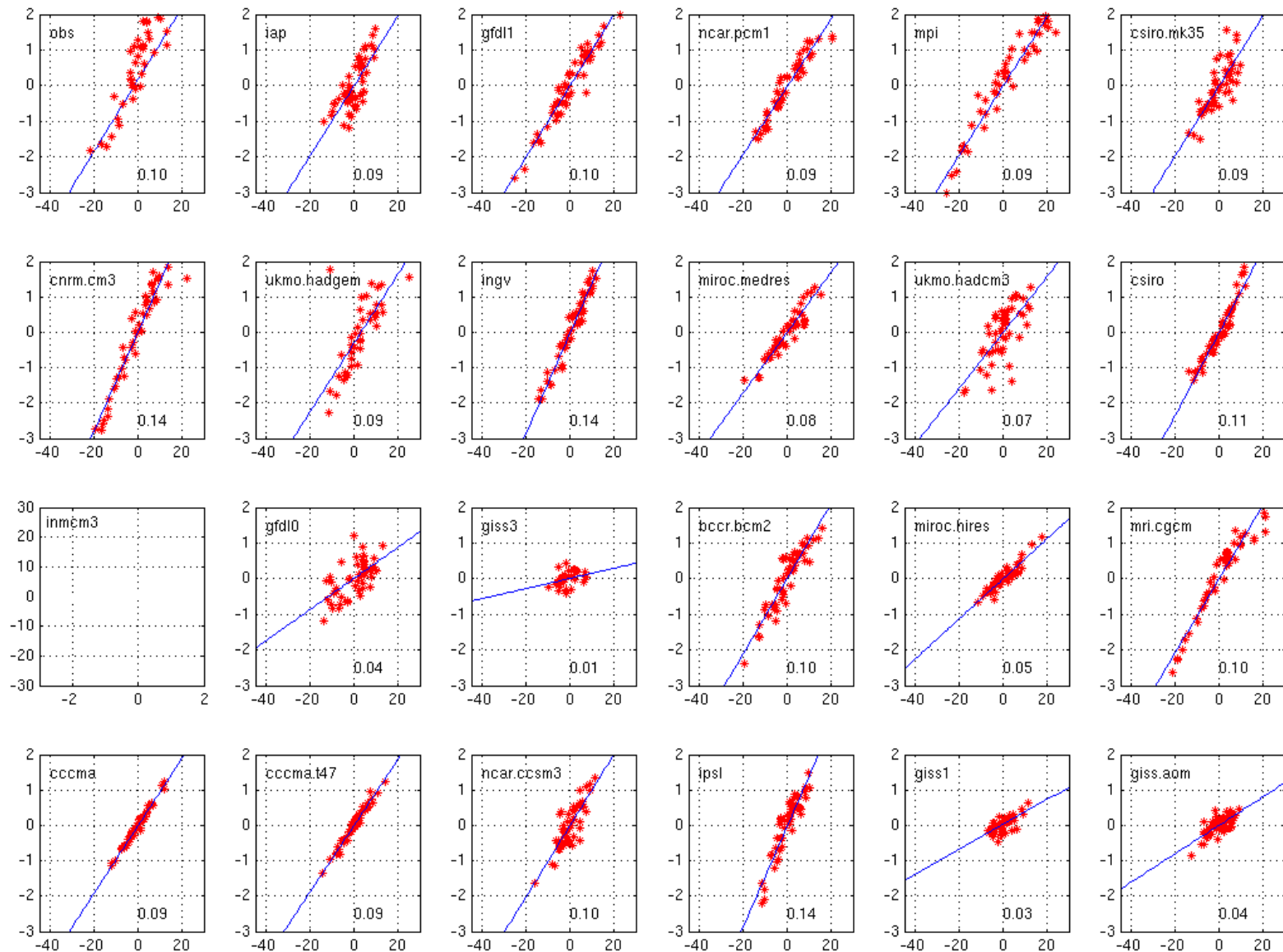
Scatter diagram between 850-hPa zonal wind anomaly in CEIO and SSTA in SEIO during the IOD developing phase (JAS) for the observation (top left) and each of the 23 AR4 models

Diagnose strength of ocean thermocline response to unit wind forcing, $R(D', u')$



Scatter diagram between thermocline depth anomaly in SEIO and 850-hPa zonal wind anomaly in CEIO

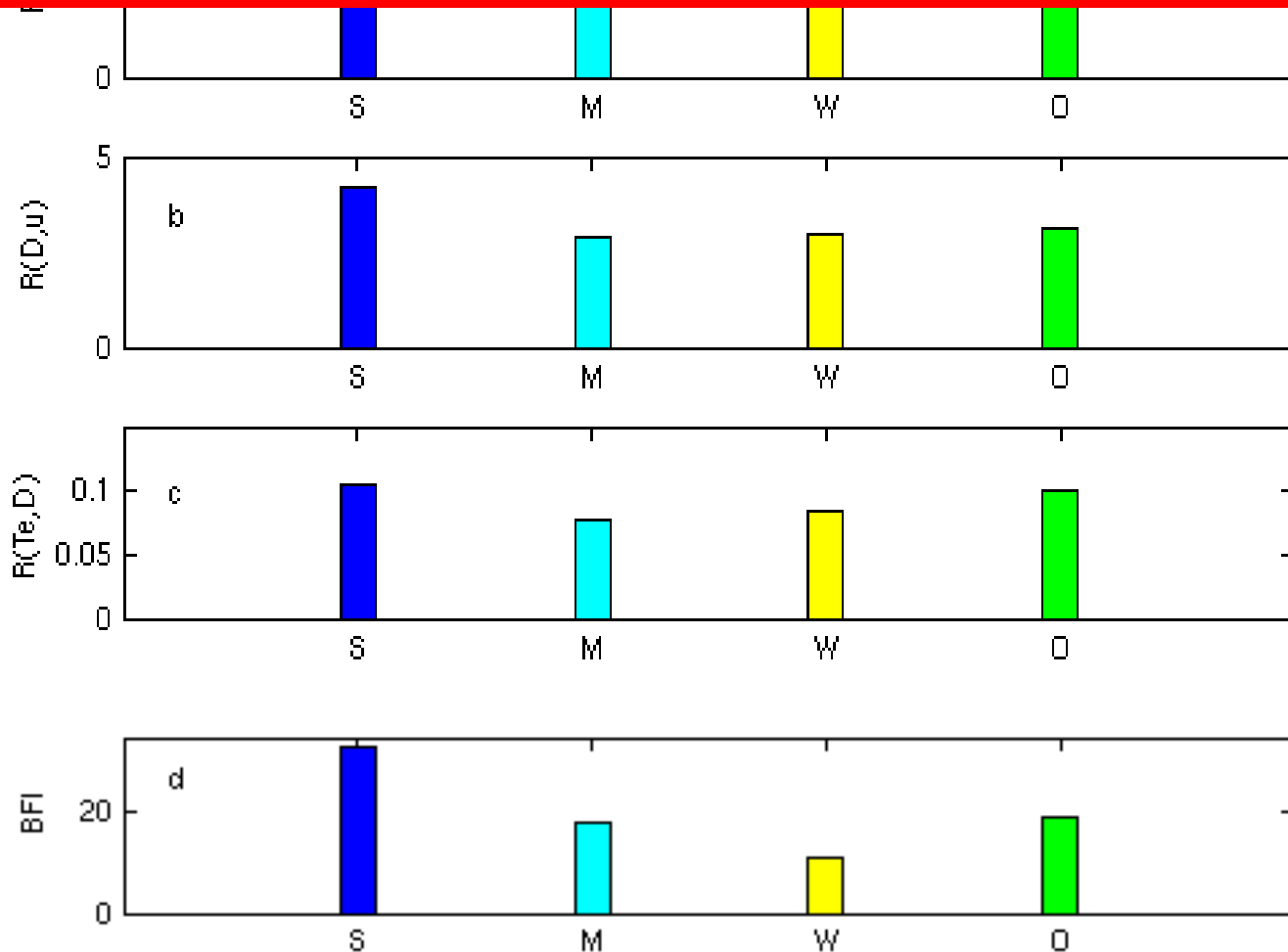
Diagnose response of subsurface temp. to unit thermocline change, $R(Te', D')$



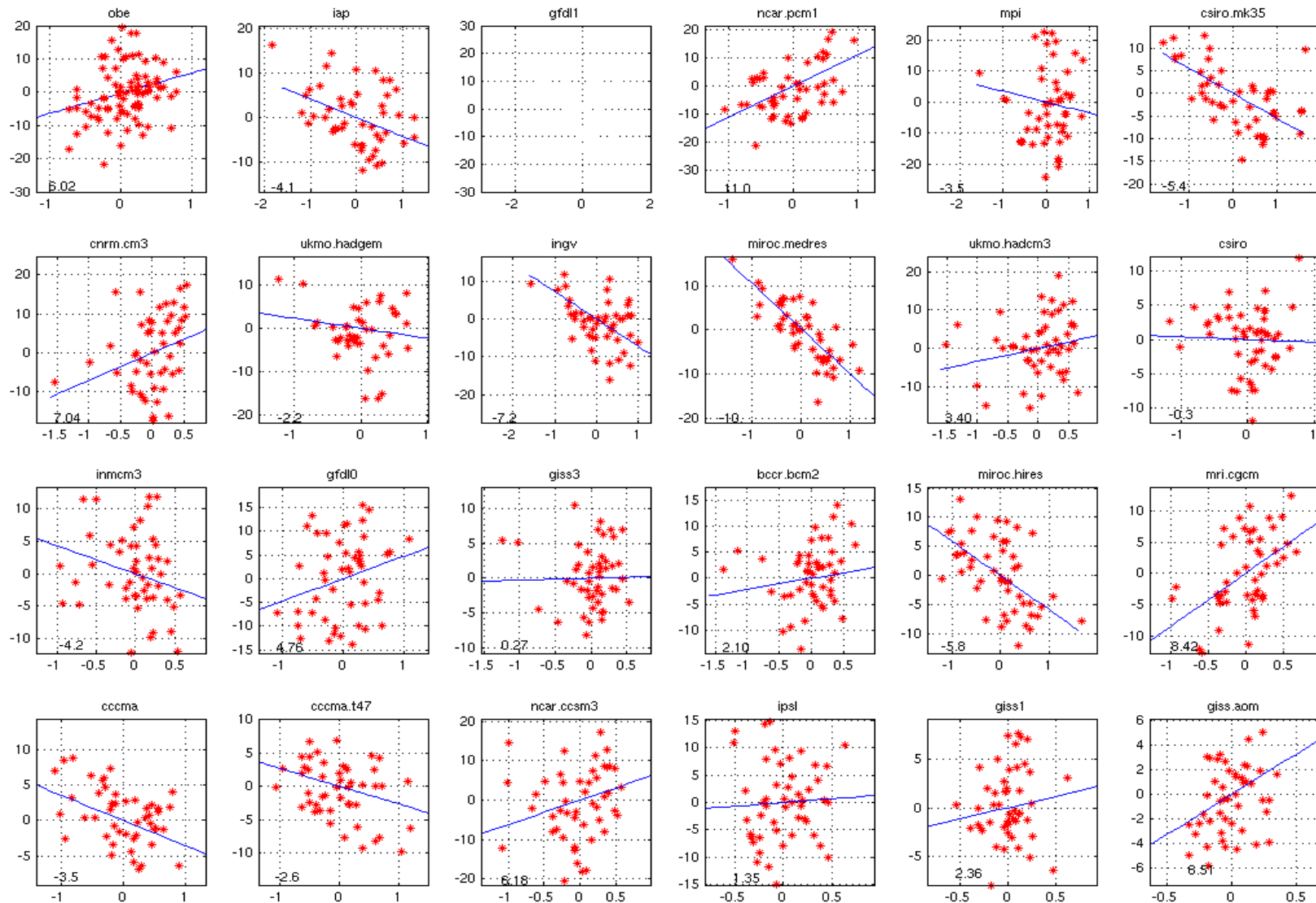
Scatter diagram between subsurface temperature anomaly and thermocline depth anomaly in SEIO

$R(u,T)$, $R(D,u)$, $R(Te,D)$ for strong, moderate and weak model groups and from the observations

$$BFI = \rho C_w \bar{w} R(u,T) R(D,u) R(Te,D)$$

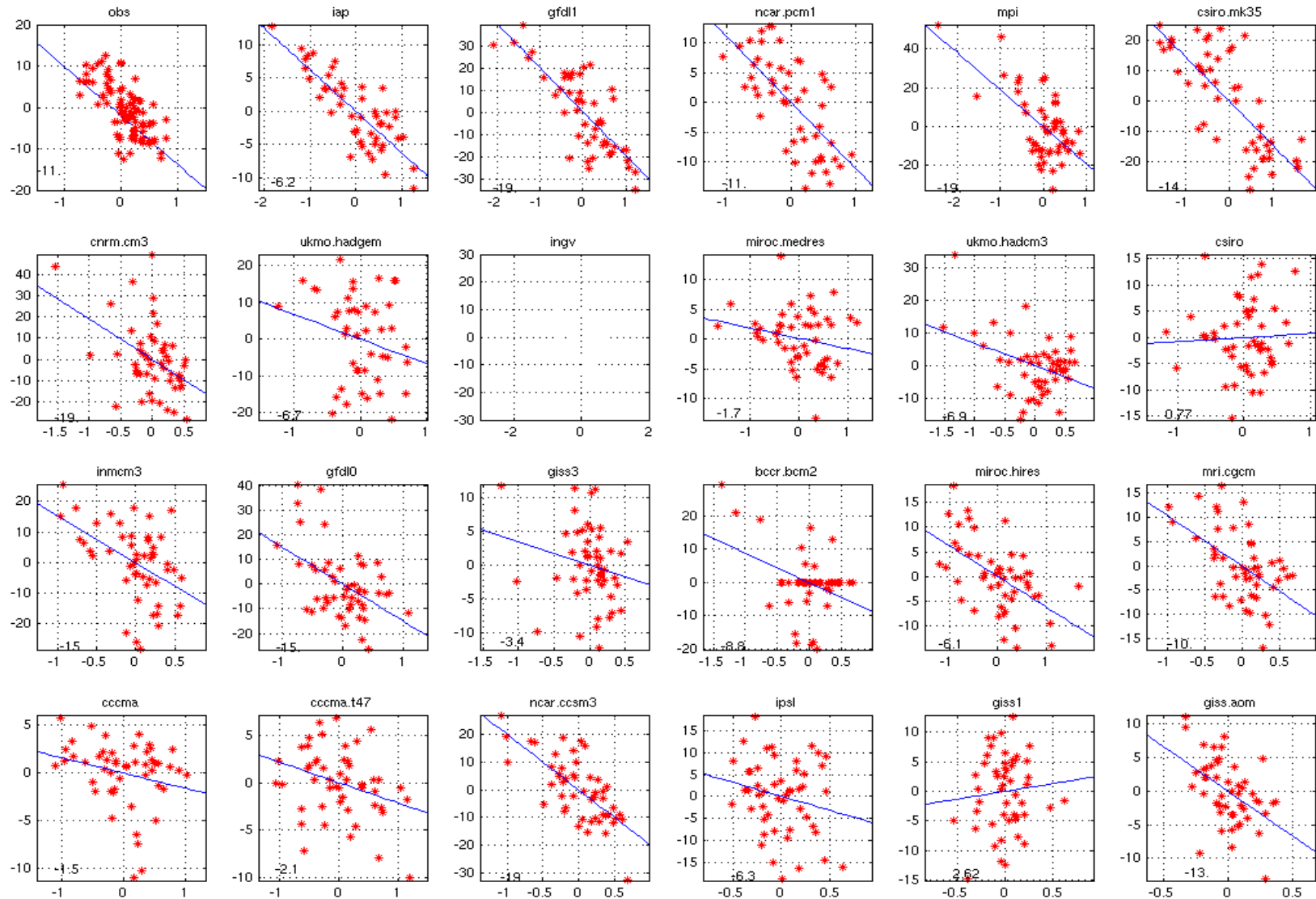


Diagnose the response of surface LHF to unit SSTA change, $R(\text{LHF}', T')$



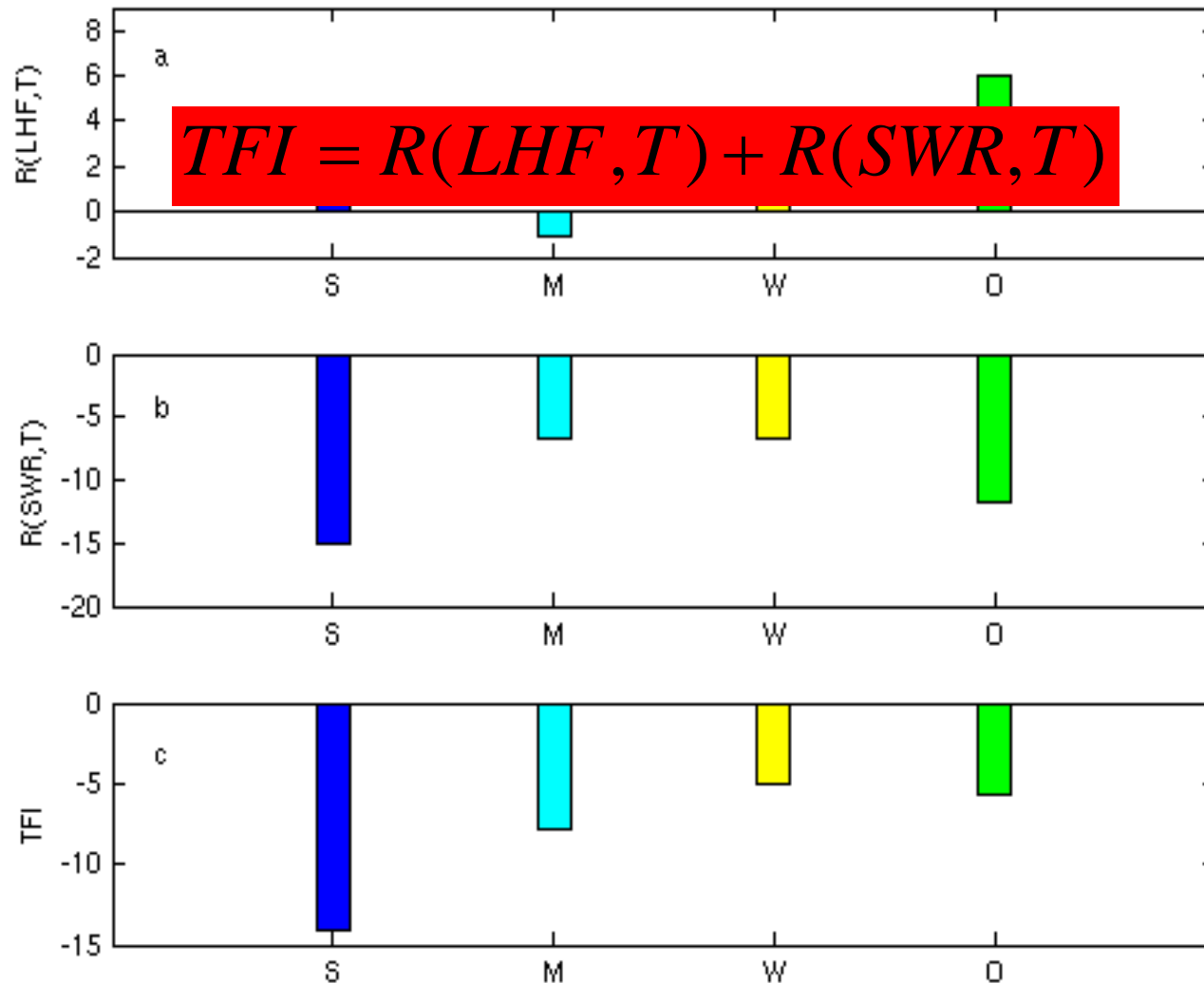
Scatter diagram between the surface latent heat flux (LHF) anomaly and SSTA in SEIO

Diagnose the response of surface SWR to unit SSTA change, $R(\text{SWR}', T')$

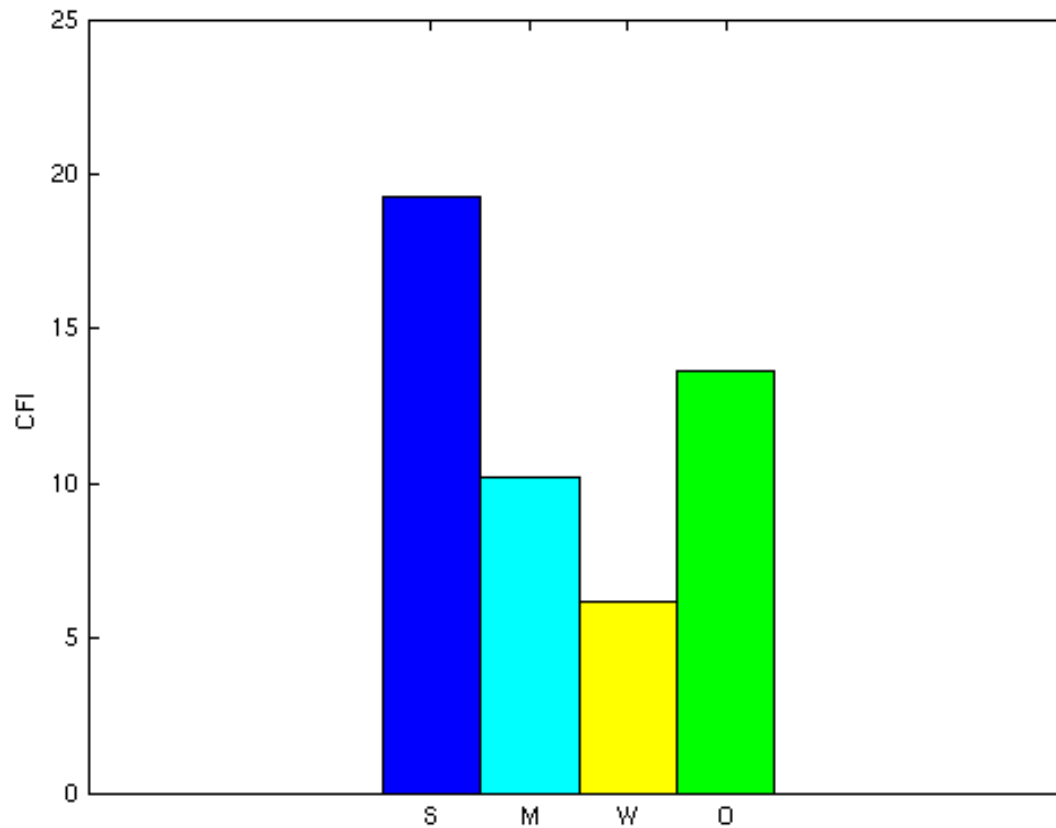


Scatter diagram between the surface net shortwave radiation anomaly and SSTA in SEIO

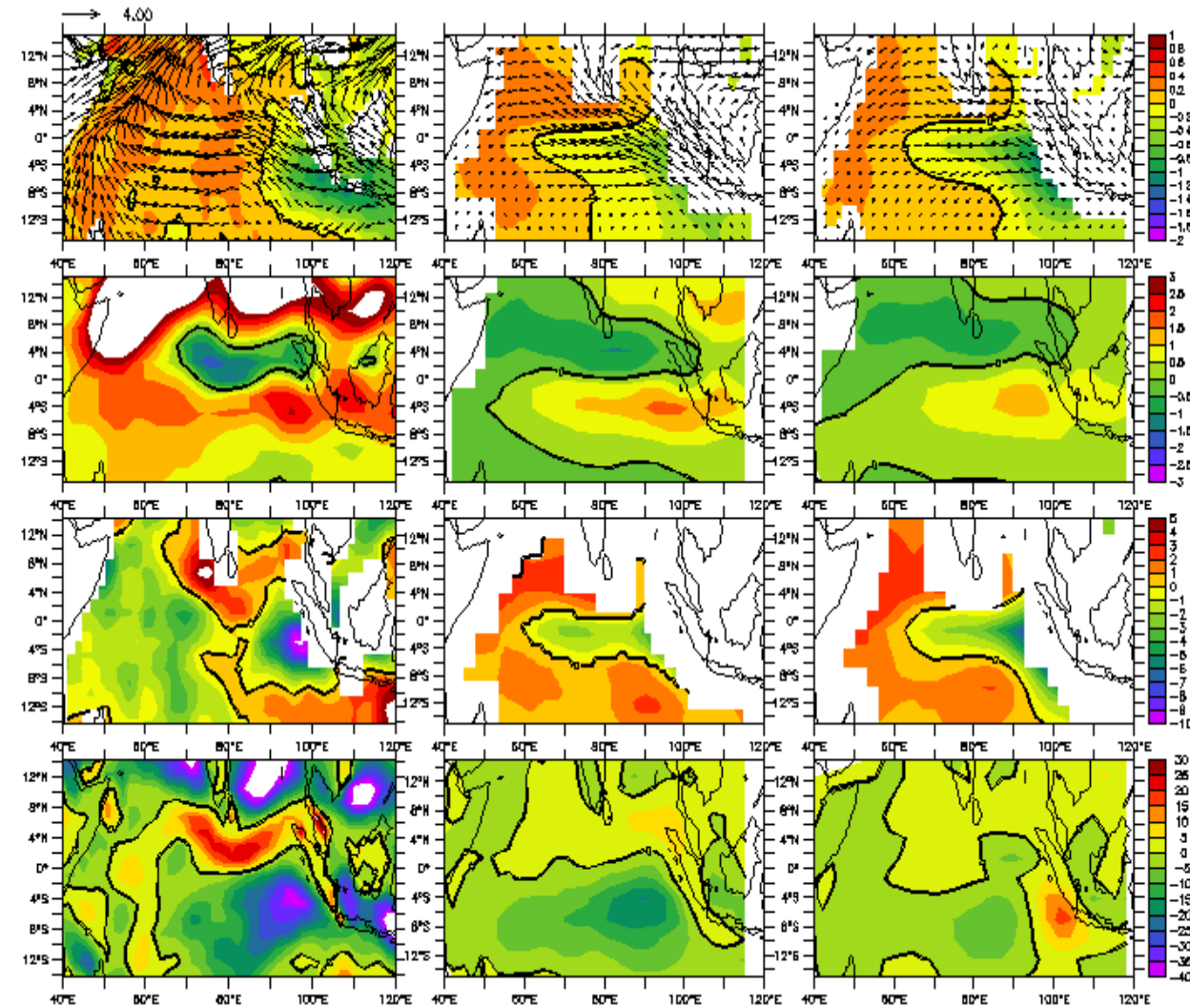
R(LHF,T) and R(SWR,T) for the strong, moderate and weak composites and from the observations



CFI during the IOD developing phase (JAS) for the strong, moderate and weak composites and from the observations



Why did some CGCMs generate a positive LHF-SST feedback while others generate a negative LHF-SST feedback?



Top: SST (shading) and 925-hPa wind (vector) anomalies

Second row: 925-hPa wind speed anomaly

Third row: sea-air specific humidity difference anomaly (qs-qa)

Bottom: surface LHF anomaly

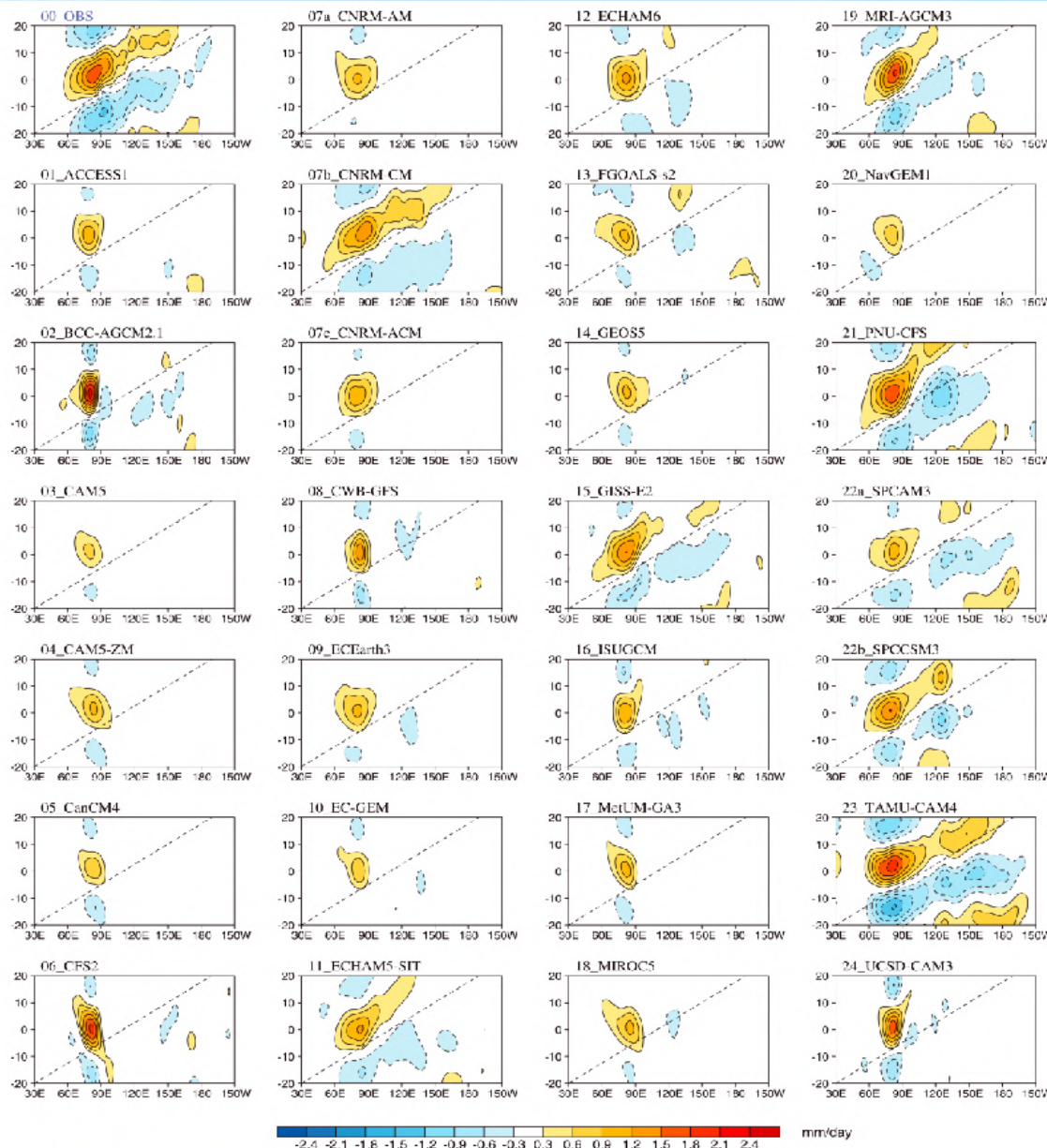
Left: observations

Middle: positive $R(\text{LHF}, T)$ model composite

Right: negative $R(\text{LHF}, T)$ model composite during IOD developing phase

Conclusion

- 23 AR4 models in simulating the Indian Ocean Dipole (IOD) were evaluated. A combined Bjerknes and thermodynamic feedback index was introduced. This index well reflects the simulated IOD strength and gives a quantitative measure of the relative contribution of the dynamic and thermodynamic feedback processes.
- The distinctive air-sea coupling strength among the AR4 models is partly attributed to the difference in the mean state. A shallower (deeper) mean thermocline, a stronger (weaker) background vertical temperature gradient, and a greater (smaller) mean vertical upwelling velocity are found in the strong (weak) simulation group. Thus, the mean state biases greatly affect the air-sea coupling strength on the inter-annual timescale.
- Many models failed to reproduce the observed positive LHF-SST feedback during the IOD development phase. The cause of this bias is attributed to the overestimate (underestimate) of effect of sea-air specific humidity (wind speed).



Lag-regression of 20-100
 day filtered rainfall with
 Indian Ocean base point
 (75E-85E; 5S-5N)

(from Jiang et al.
 2015)

Science Question: What is the key mechanism for distinctive
 propagating features among GCMs?

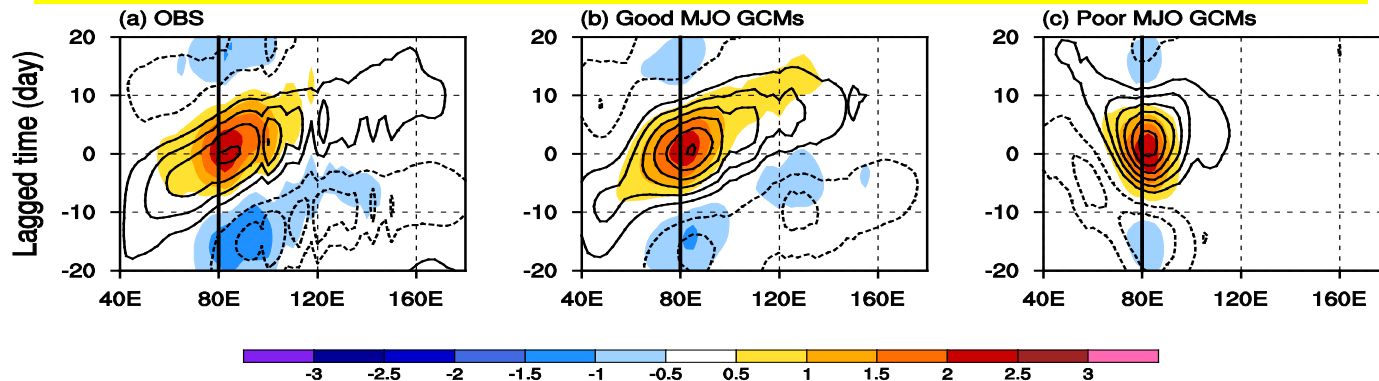
Column integrated Moist Static Energy (MSE) budget

MSE $m = c_p T + gz + Lq$

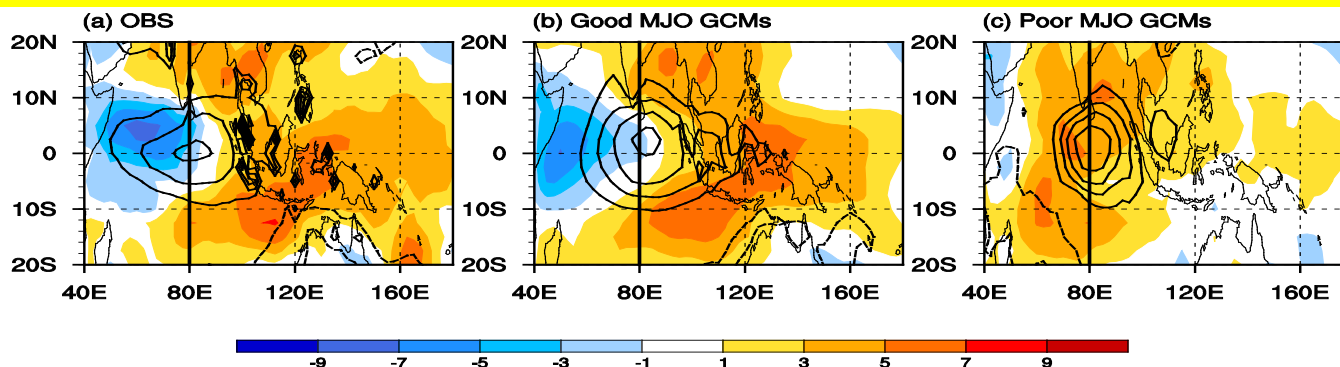
Column MSE budget $\langle \partial_t m \rangle = - \langle \omega \partial_p m \rangle - \langle \vec{V} \cdot \nabla m \rangle + Q_t + Q_r$

< >: mass-weighted vertical integration from surface to 100 hPa

<MSE> (contour) and rainfall (shaded) over 10S-10N



<MSE> (contour) & <MSE> tendency (shaded) at Day 0



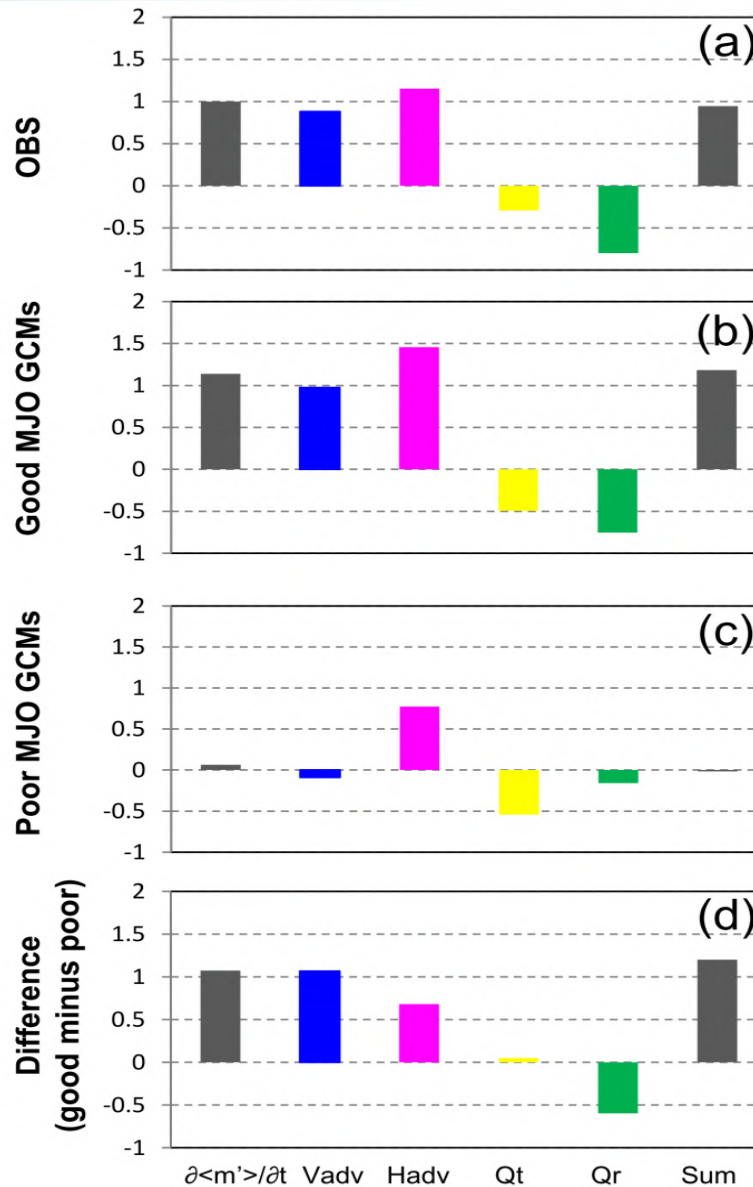
Projecting each MSE budget term to observed MSE tendency over (40° -160° E, 10° S-10° N)

OBS

Good

Poor

Good — poor



Projection method following Anderson and Kuang (2011)

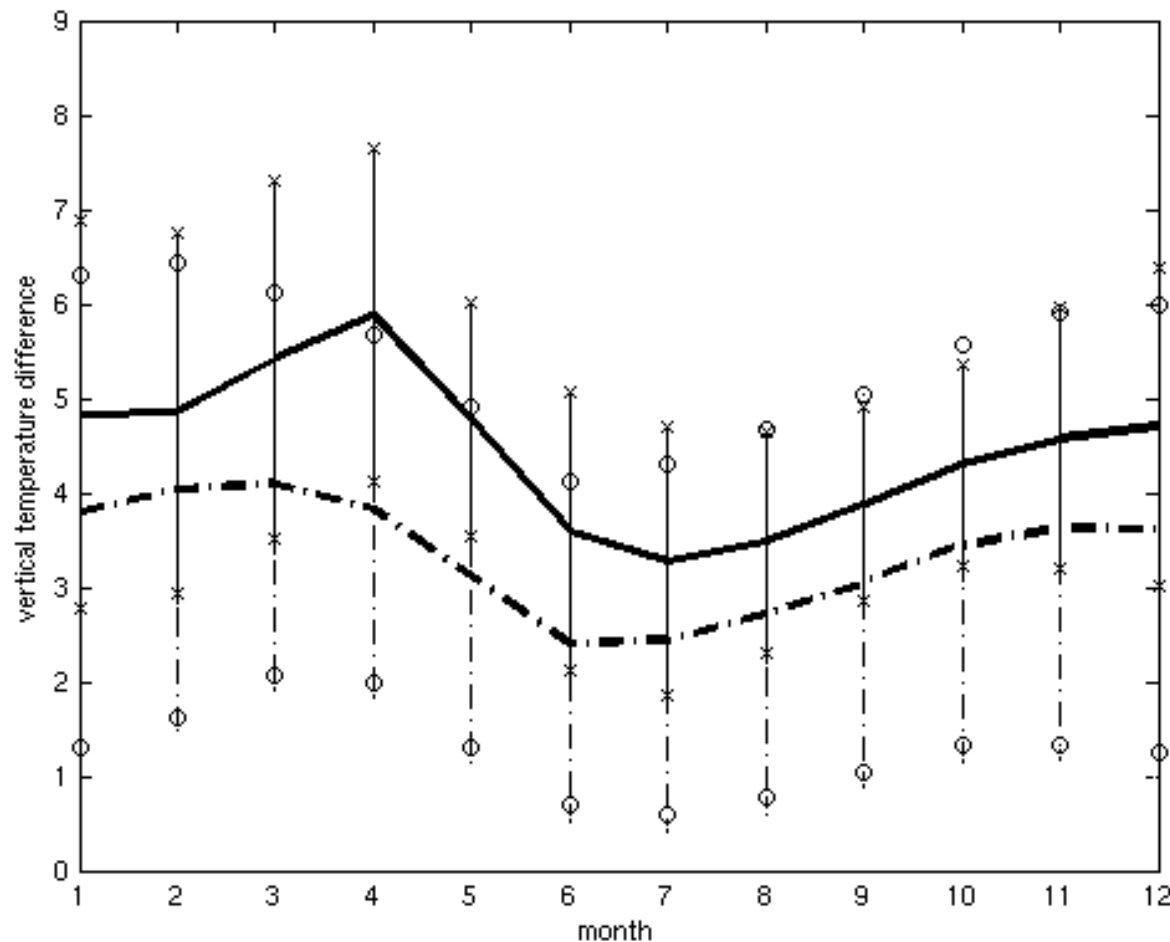
Thanks

Diamond Head

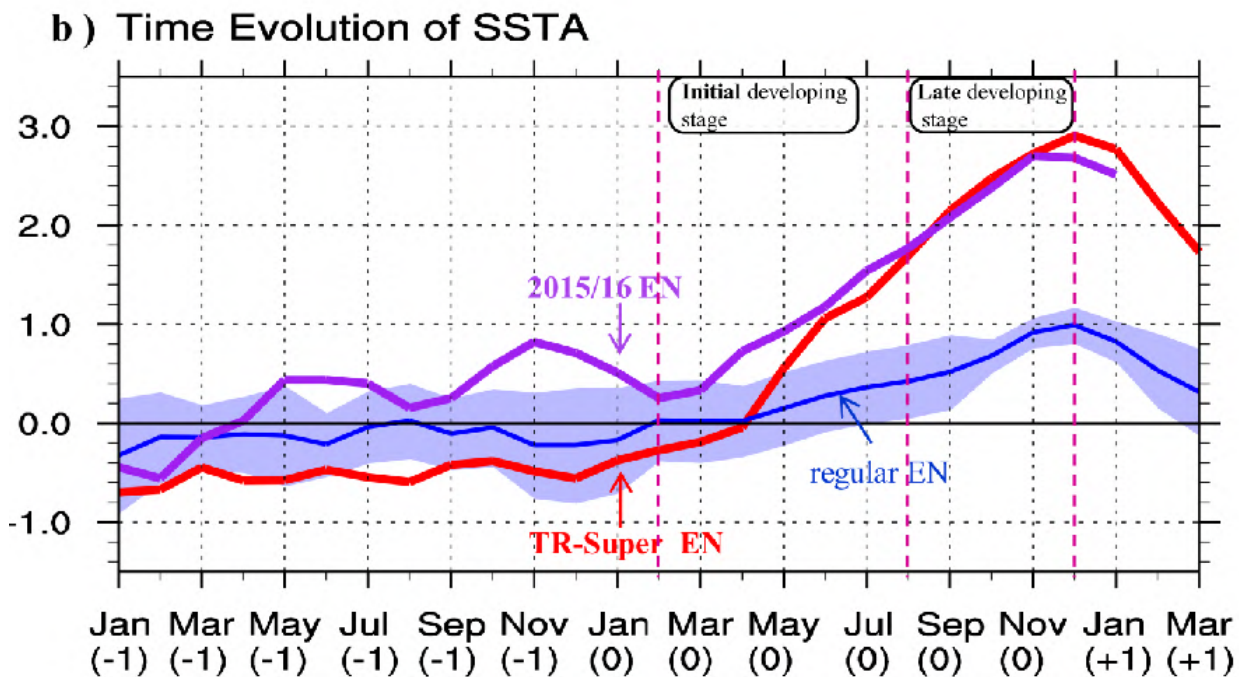
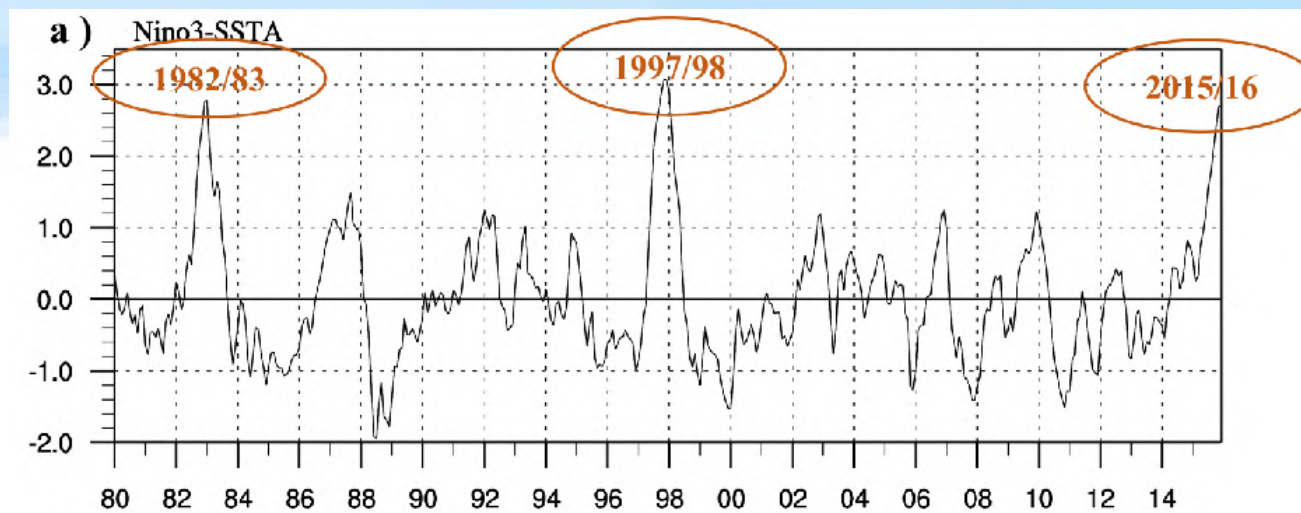


Mean state difference between strong and weak groups:

- 1) mean thermocline depth along the equator
- 2) mean w
- 3) upper-ocean vertical temperature gradient

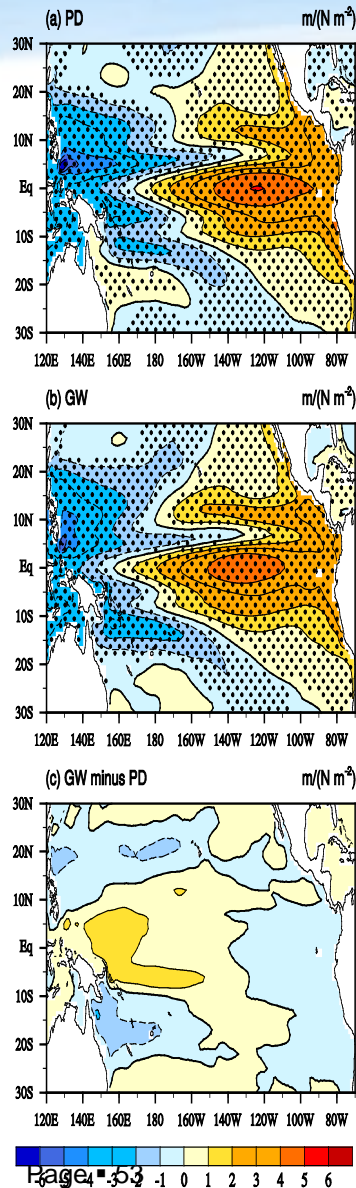


$$w' \frac{\partial \bar{T}}{\partial z}$$

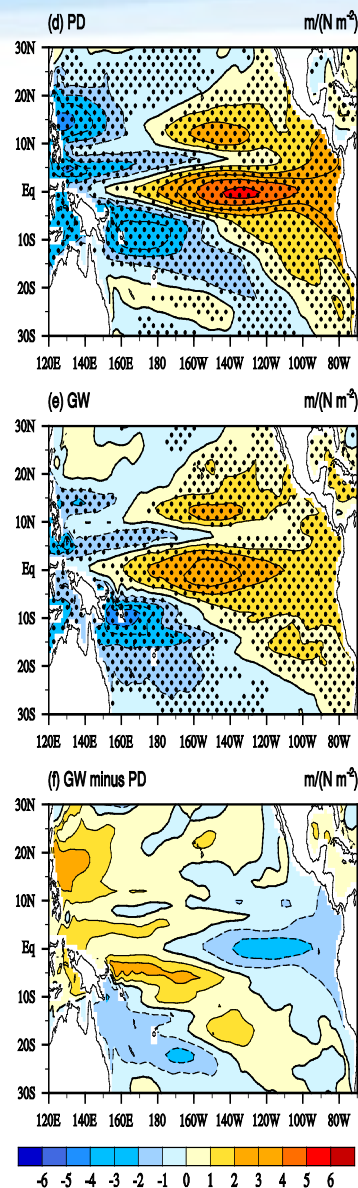


Thermocline-depth patterns regressed onto Nino4 Taux anomaly

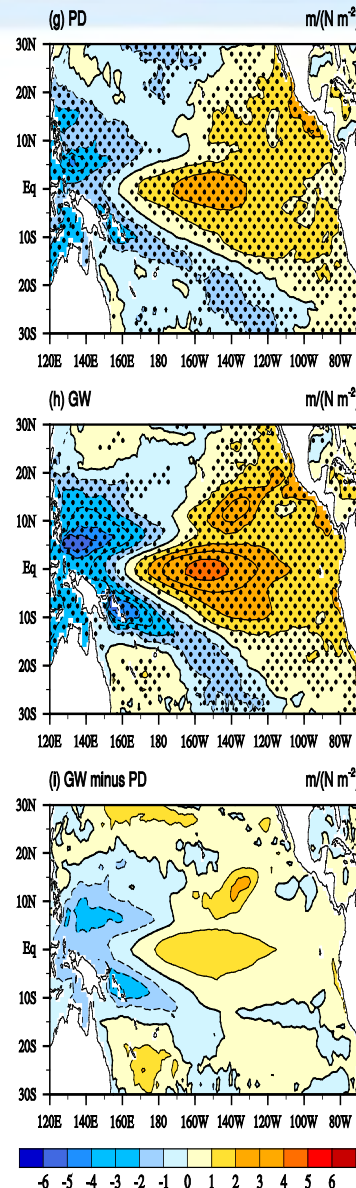
CCSM4



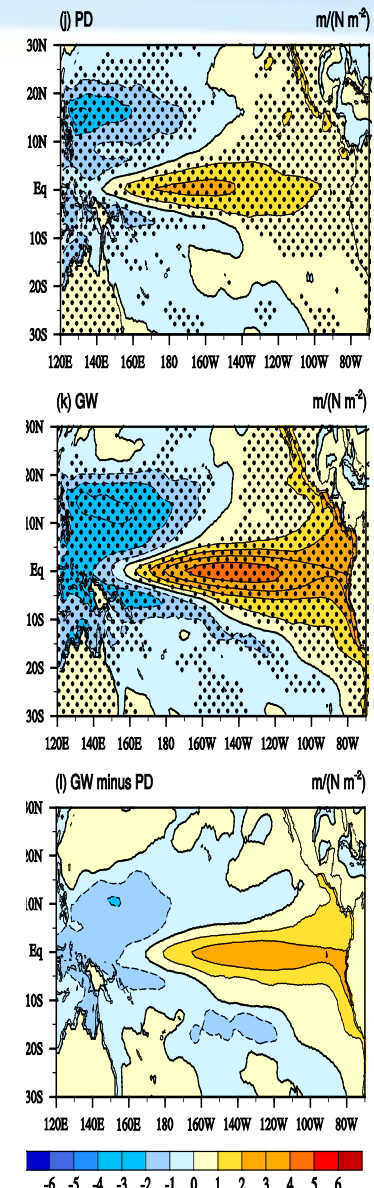
FGOALS-g2



MPI-ESM-MR



MRI-CGCM3



PD

GW

GW —
PD

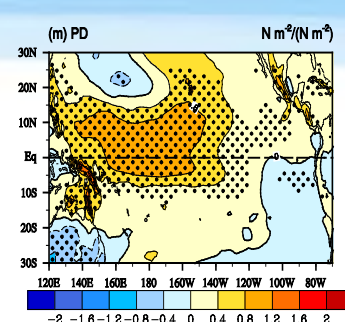
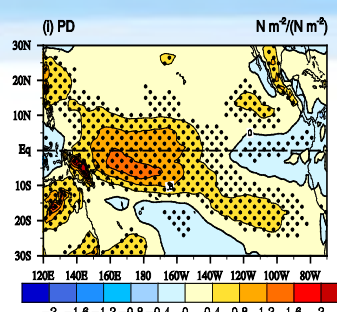
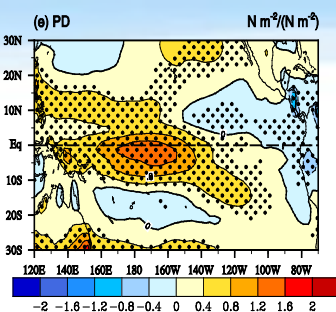
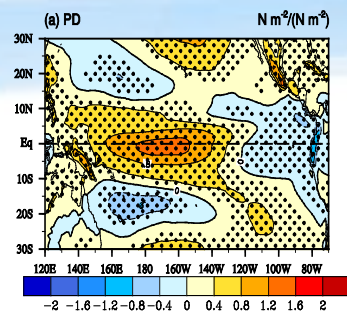
What causes distinctive TH responses ? → Change of meridional profile of Taux'

CCSM4

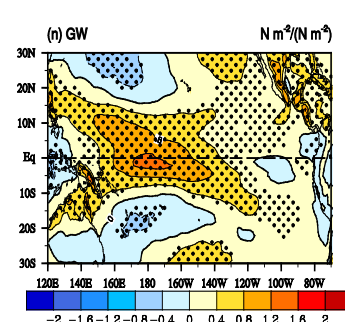
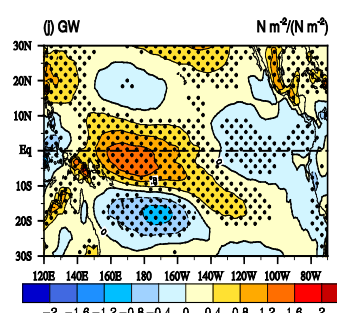
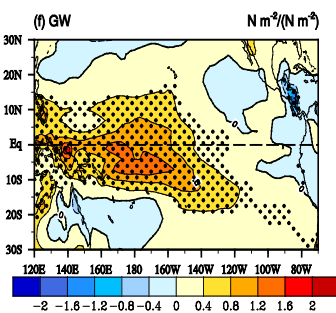
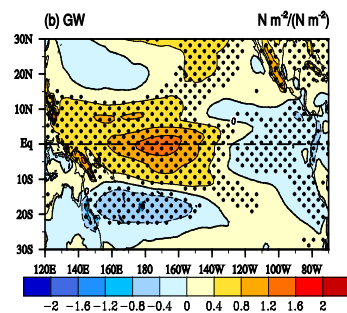
FGOALS-g2

MPI-ESM-MR

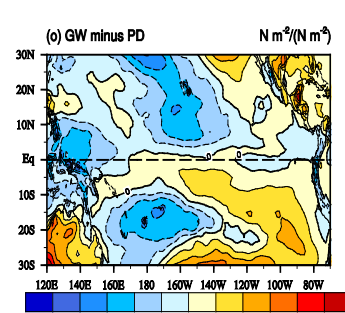
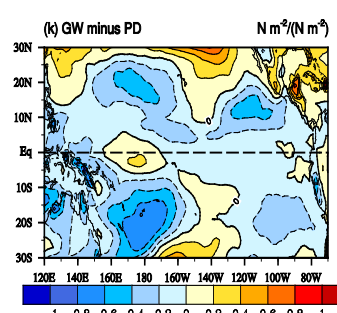
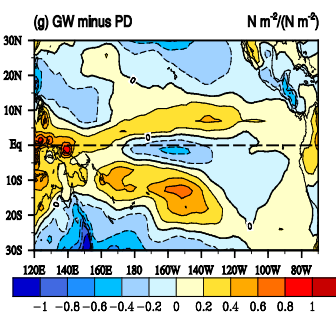
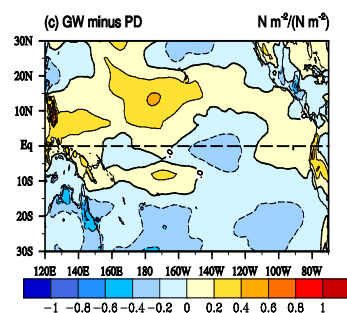
MRI-CGCM3



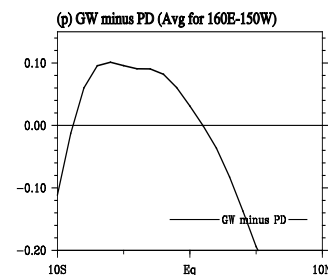
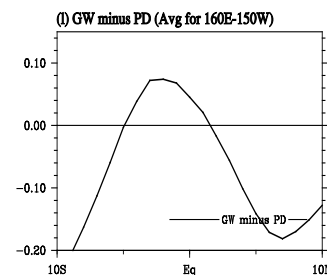
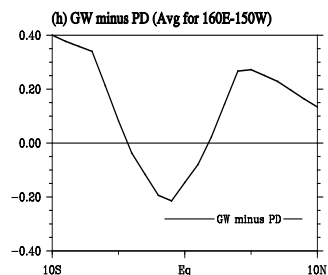
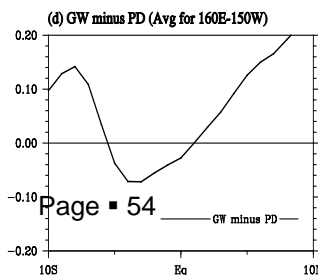
PD



GW



GW — PD

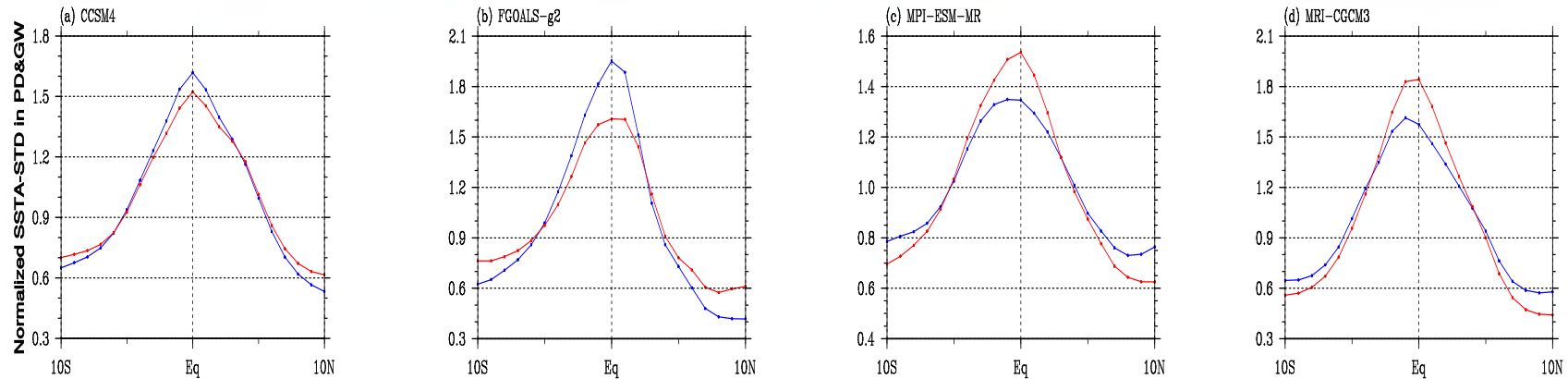


Taux'
regressed
onto Nino4
Taux' index

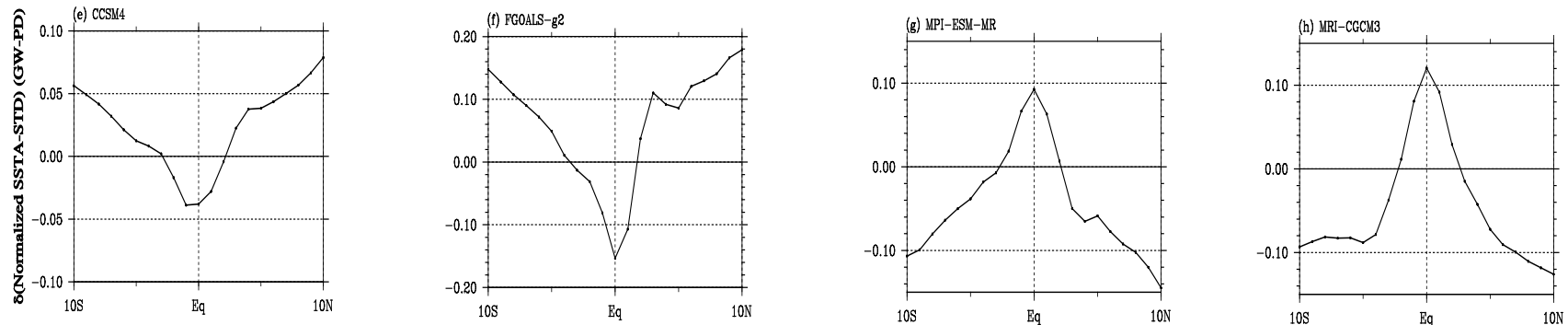
Change of Meridional Width of SSTA

SSTA-Std regressed onto the Nino3 index

— PD — GW

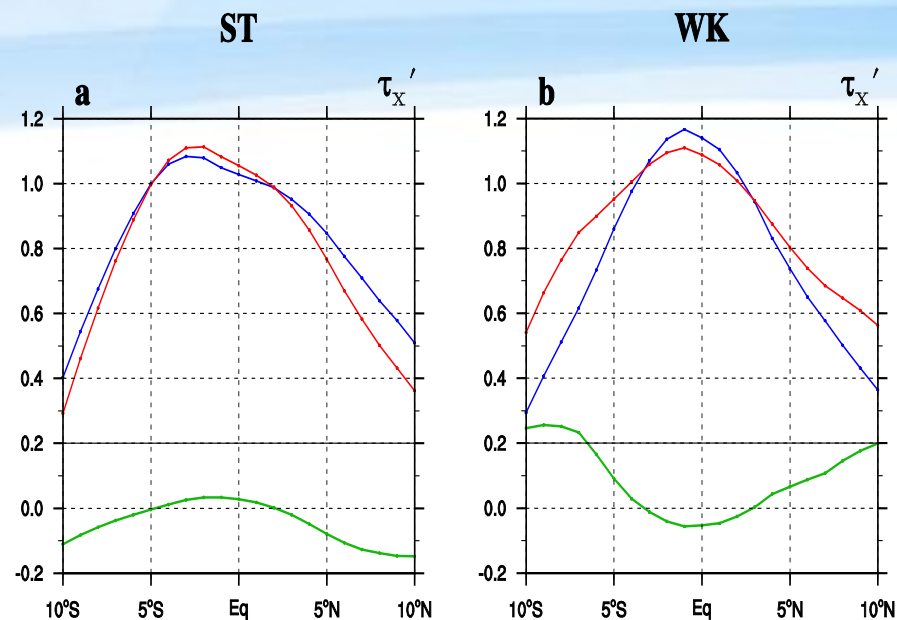


— (GW—PD)



→ Decreased (increased) meridional scale of TauxA and SSTA was found in the CGCMs with strengthened (weakened) ENSO amplitude.

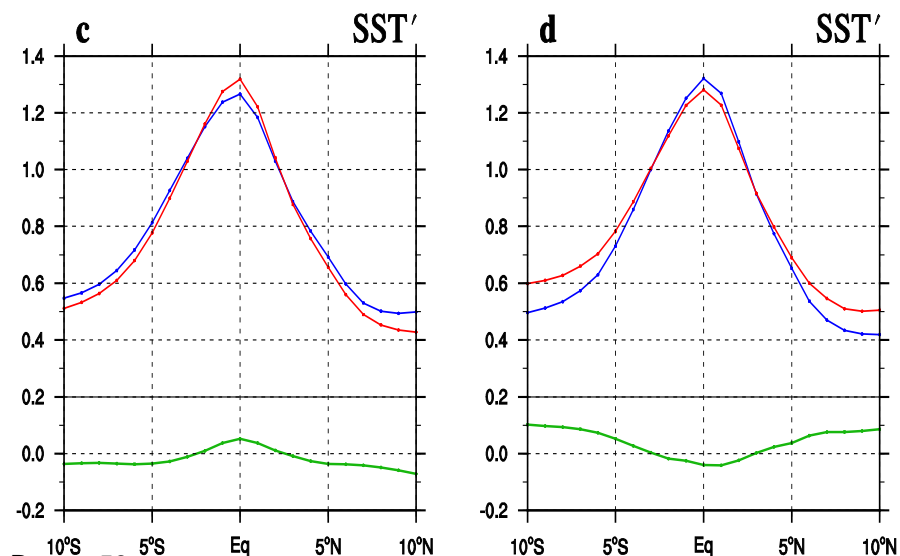
Meridional Structure Change of **Taux'** and **SSTA** in 20 CMIP5 Models



(**Top**) Regressed **Taux'** averaged over 160°E-150°W for ST and WK groups

(**Bottom**) Regressed **SSTA** averaged over 150°W-90°W.

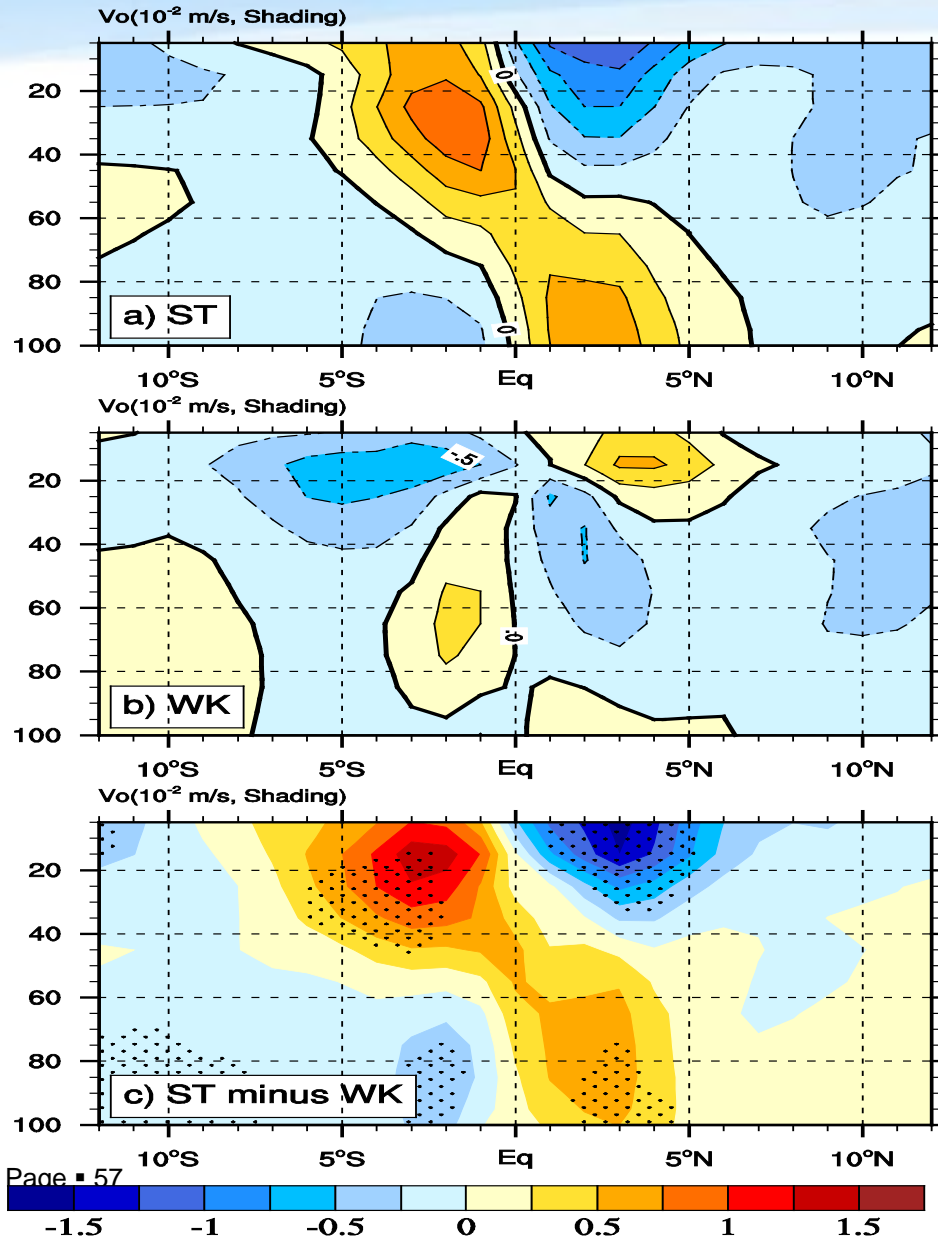
Blue: PD; Red: GW; Green: GW-PD



➔ In the **ST** (**WK**) group, **Taux'** and **SSTA** patterns become more **sharp** (**flat**) in their meridional structures under GW.

Changes of the Mean STC Intensity (ST vs. WK Group)

Meridional Ocean Current Change



(Left) Composite meridional ocean current change averaged over 160E-90W for **ST** (top) and **WK** (middle) groups and **their difference** (bottom, **ST minus WK**)

The **stippling** in the bottom panel indicates that the difference exceeds a **95% confidence level** using Student's t-test.

Conclusion

- **ENSO amplitude changes in 20 CMIP5 models are primarily controlled by Bjerknes TH and ZA feedback changes, both of which are determined by distinctive changes of TH response to unit wind stress forcing.**
- **The change of the mean state does not directly affect ENSO amplitude change but does indirectly affect it through the change of mean Subtropical Cell, which affects the meridional width of ENSO and thus coupled air-sea feedback strength.**